Since January 2020 Elsevier has created a COVID-19 resource centre with free information in English and Mandarin on the novel coronavirus COVID-19. The COVID-19 resource centre is hosted on Elsevier Connect, the company's public news and information website.

Brain, Behavior, and Immunity 91 (2021) 159–171

Contents lists available at ScienceDirect

Brain, Behavior, and Immunity

journal homepage: www.elsevier.com/locate/ybrbi

Lung pathology due to hRSV infection impairs blood–brain barrier permeability enabling astrocyte infection and a long-lasting inflammation in the CNS

Karen Bohmwald[a], Jorge A. Soto[a], Catalina Andrade-Parra[a], Ayleen Fernández-Fierro[a], Janyra A. Espinoza[a], Mariana Ríos[a], Eliseo A. Eugenin[c], Pablo A. González[a], María Cecilia Opazo[b], Claudia A. Riedel[b,*], Alexis M. Kalergis[a,d,*]

[a] Millennium Institute on Immunology and Immunotherapy, Departamento de Genética Molecular y Microbiología, Facultad de Ciencias Biológicas, Pontificia Universidad Católica de Chile, Chile
[b] Millennium Institute on Immunology and Immunotherapy, Departamento de Ciencias Biológicas, Facultad de Ciencias de la Vida, Universidad Andres Bello, Santiago, Chile
[c] Department of Neuroscience and Cell Biology, The University of Texas Medical Branch, Galveston, TX 77555, United States
[d] Departamento de Endocrinología, Facultad de Medicina, Pontificia Universidad Católica de Chile, Chile

ARTICLE INFO

Keywords:
Human respiratory syncytial virus
Central nervous system
Inflammation
Astrocytes
Behavior alteration

ABSTRACT

The human respiratory syncytial virus (hRSV) is the most common infectious agent that affects children before two years of age. hRSV outbreaks cause a significant increase in hospitalizations during the winter season associated with bronchiolitis and pneumonia. Recently, neurologic alterations have been associated with hRSV infection in children, which include seizures, central apnea, and encephalopathy. Also, hRSV RNA has been detected in cerebrospinal fluids (CSF) from patients with neurological symptoms after hRSV infection. Additionally, previous studies have shown that hRSV can be detected in the lungs and brains of mice exposed to the virus, yet the potential effects of hRSV infection within the central nervous system (CNS) remain unknown. Here, using a murine model for hRSV infection, we show a significant behavior alteration in these animals, up to two months after the virus exposure, as shown in marble-burying tests. hRSV infection also produced the expression of cytokines within the brain, such as IL-4, IL-10, and CCL2. We found that hRSV infection alters the permeability of the blood–brain barrier (BBB) in mice, allowing the trespassing of macromolecules and leading to increased infiltration of immune cells into the CNS together with an increased expression of pro-inflammatory cytokines in the brain. Finally, we show that hRSV infects murine astrocytes both, *in vitro* and *in vivo*. We identified the presence of hRSV in the brain cortex where it colocalizes with vWF, MAP-2, Iba-1, and GFAP, which are considered markers for endothelial cells, neurons, microglia, and astrocyte, respectively. hRSV-infected murine astrocytes displayed increased production of nitric oxide (NO) and TNF-α. Our results suggest that hRSV infection alters the BBB permeability to macromolecules and immune cells and induces CNS inflammation, which can contribute to the behavioral alterations shown by infected mice. A better understanding of the neuropathy caused by hRSV could help to reduce the potential detrimental effects on the CNS in hRSV-infected patients.

1. Introduction

The human respiratory syncytial virus (hRSV) is currently the primary cause of acute respiratory tract infections (ARTIs) worldwide (Calvo et al., 2008; Divarathne et al., 2019; Obodai, 2018). hRSV infection is characterized by a wide range of symptoms including low-grade fever, cough, rhinorrhea, congestion, otitis and more severe manifestations, such as bronchiolitis and pneumonia (Sweetman et al.,

* Corresponding authors at: Millennium Institute on Immunology and Immunotherapy, Departamento de Ciencias Biológicas, Facultad de Ciencias de la Vida, Universidad Andres Bello, República #440, Santiago 8331010, Chile (C.A. Riedel). Millennium Institute on Immunology and Immunotherapy. Departamento de Genética Molecular y Microbiología, Facultad de Ciencias Biológicas, Pontificia Universidad Católica de Chile, Avenida Libertador Bernardo O'Higgins #340, Santiago 8331010, Chile (A.M. Kalergis).
E-mail addresses: claudia.riedel@unab.cl (C.A. Riedel), akalergis@bio.puc.cl, akalergis@icloud.com (A.M. Kalergis).

https://doi.org/10.1016/j.bbi.2020.09.021
Received 9 April 2020; Received in revised form 30 August 2020; Accepted 17 September 2020
Available online 24 September 2020

2005). Although most symptoms of hRSV infection are associated with pulmonary pathology, other tissues may also be affected by this virus, such as the central nervous system (CNS) (Eisenhut, 2007, 2006; Kawashima et al., 2009, 2012; Kho et al., 2004; Millichap and Wainwright, 2009; Morichi et al., 2011, 2017). Both, in humans and animal models it has been observed that after exposure to hRSV, disease manifestations can involve the CNS (Millichap and Wainwright, 2009; Picone et al., 2019; Espinoza et al., 2013). Indeed, a proportion of patients with hRSV-associated severe bronchiolitis can develop neurological abnormalities, such as seizures (Kho et al., 2004; Ng et al., 2001; Cha et al., 2019), central apnea (Kho et al., 2004); lethargy, (Sweetman et al., 2005; Kho et al., 2004) feeding or swallowing difficulties (Sweetman et al., 2005; Kho et al., 2004), strabismus (Antonucci and Fanos, 2005), encephalopathy (Eisenhut, 2007; Millichap and Wainwright, 2009; Picone et al., 2019; Bohmwald et al., 2014, 2018), and elevated cytokines levels or increased cellularity in the cerebrospinal fluid (CSF) (Kawashima et al., 2012; Kho et al., 2004; Otake et al., 2007). Additionally, studies in rodents have shown that hRSV can cause cognitive alterations, similarly to what has been reported for the other respiratory viruses, such as the influenza virus and SARS-CoV-2 (Jurgens et al., 2012; Jang et al., 2009; Mao et al., 2020; Meinhardt, 2020; Moriguchi et al., 2020; Bernard-Valnet, 2020; Hornuss, 2020; Rogers et al., 2020). These observations suggest that hRSV could alter the proper function of the CNS. However, the cellular and molecular mechanisms involved in these processes remain poorly understood (Eisenhut, 2006; Kho et al., 2004; Morichi et al., 2011).

Although the pathophysiological basis for hRSV-related encephalopathy remains unknown, numerous studies support a link between hRSV-caused neurological components of host inflammatory response (Kawashima et al., 2009, 2012; Morichi et al., 2017; Otake et al., 2007). Cytokine measurements in the CSF from patients suffering hRSV-associated encephalopathy have shown increased levels of pro-inflammatory for IL-6, IL-8, CCL2 and CCL4 (Eisenhut, 2007; Kawashima et al., 2012; Morichi et al., 2017). Importantly, while IL-6 is usually involved in detrimental inflammatory processes (Kawashima et al., 2012; Tanaka et al., 2014), IL-8, CCL2, and CCL4 are associated with the recruitment of immune cells to the tissues where these molecules are present (Griffith et al., 2014).

Currently, two models have been proposed for explaining as to how hRSV could alter the CNS function: the first consist of an indirect effect as a consequence of peripheral viral replication leading to inflammation and the second through a direct effect mediated by hRSV infection of the CNS and local inflammation induced by the virus. These two models are not mutually exclusive. A previous study carried out by our group found evidence of hRSV proteins in the brain of mice at three days post-infection (Espinoza et al., 2013). In addition, behavioral and spatial learning impairment were shown by hRSV-infected mice and rats, even several days after the infection was resolved (Espinoza et al., 2013; Céspedes et al., 2017).

To gain a better understanding of the mechanisms involved in hRSV-caused behavioral alterations, here we assessed whether hRSV infection can lead to an inflammatory response in the CNS. We found that hRSV-infected mice displayed behavioral alterations that extended at up to 60 days post-infection (p.i.). We were able to identify the presence of hRSV proteins localizing with astrocytes at the brain cortex of these mice. Moreover, our results suggest that hRSV infection alters the permeability of the blood–brain barrier (BBB) and significantly increases the number of CNS-infiltrating inflammatory monocytes, B lymphocytes and $CD8^+$ T cells. Further, the local expression of pro-inflammatory cytokines, such as IL-6 and TNF-α, was increased in the CNS of infected mice. Importantly, endothelial cells, neurons, microglia and astrocytes were shown to be infected with hRSV *in vivo*. Because the infection was more frequent in astrocytes as compared to the other cell types, we analyzed hRSV infection of astrocytes *in vitro*, observing an increased expression of the glial fibrillary acidic protein (GFAP) in these cells. Furthermore, we evaluated if the inflammation in the CNS due to hRSV infection could lead to behavioral alterations in mice. These data support the notion that hRSV can reach the CNS altering BBB permeability, infecting astrocytes and activating them leading to local inflammation within the CNS that can contribute to the long-term behavioral and cognitive alterations.

2. Material and methods

2.1. Ethics statement

All mouse experiments were conducted in agreement with ethical standards and according to the national (Chile) animal protection law number 20.800. All experimental protocols were carried out according to the Sanitary Code of Terrestrial Animals of the World Organization for Animal Health (OIE, 24ª Edition, 2015) and were reviewed and approved by the Scientific Ethical Committee for Animal and Environment Care of the Pontificia Universidad Católica de Chile (Protocol number CBB-120/2014).

2.2. Mice

Initial colonies of BALB/cJ mice were obtained from Jackson Laboratory and mice were subsequently bred at the Pontificia Universidad Católica de Chile facility. Female mice used for *in vivo* experiments were 4- to 6-weeks old and 1–3 postnatal days old for astrocyte primary cell cultures. In order to avoid differences due to gender, only female mice were included in these experiments, since a previous study showed that the phenotype of interest was observed more clearly in female mice (Espinoza et al., 2013).

2.3. Virus production

HEp-2 cell line (ATCC® CCL-23™) was used to propagate the hRSV serogroup A2, strain 13018–8, a clinical isolate provided by the Public Health Institute of Chile. Briefly, HEp-2 monolayers were grown in a T75 flask with DMEM (IThermofisher, Carlsbad, CA) supplemented with 10% FBS (Thermofisher, Carlsbad, CA). Flasks containing 5 ml of culture medium were inoculated at Multiplicity of Infection (MOI) equal to 1 for hRSV and incubated at 37 °C. After viral adsorption (2 h), the culture medium was replaced for fresh DMEM 1% FBS and incubated for 48 h or until the visible cytopathic effect was observed. The flask content was pooled and spun once at 300xg for 5 min to remove cell debris. In parallel, supernatants were recollected from non-infected HEp-2 cells monolayers and used as uninfected control (mock). The UV-hRSV (as UV-inactivated hRSV control) was obtained by the exposure of hRSV vial to ultraviolet light for 30 min. Viral titles of supernatants were determined by immunohistochemistry as it was described by Gómez *et al.* (Gomez, 2016). Briefly, infectious supernatants were serially diluted (10-fold dilutions) and added over 96-well plates with HEp-2 monolayers (at 80% confluence), and incubated for 48 h at 37 °C. After, the cells were fixed with 2% PFA-PBS. Extracellular staining was done with the anti-F-hRSV (Palivizumab)-HRP antibody for 1 h (20 μg/ml). After two washes with PBS, the substrate TRUE-BLUE Peroxidase was added and incubated for 10 min at RT. Plaques formation and hRSV syncytia were observed in an optical microscope and quantified.

2.4. hRSV challenge in vivo

Four to six weeks old female BALB/cJ mice were anesthetized intraperitoneally (i.p.) with a dose of ketamine/xylazine (20 mg/kg and 1 mg/kg, respectively) and challenged intranasally (i.n.) with $1x10^6$ PFU of hRSV (13018–8 strain) or UV-hRSV or mock (as non-infectious control). Animal body weight was recorded until 7 days p.i. (Espinoza et al., 2013).

2.5. Marble burying tests

To evaluate the digging behavior of infected and control mice, the marble burying test (MB) was performed in accordance with (Deacon, 2006). The MB test allows to evaluate a spontaneous and natural behavior of mice that reflects the function of the ventral hippocampus (Deacon and Rawlins, 2005; Wang, 2019). The advantages of using the MB test are the simplicity and robustness of the data, along with the absence of pain and suffering imposed to the experimental animals (Deacon, 2009). Briefly, animal cages were filled with approximately 5 cm of wood chip bedding, lightly tamped down to make a flat and uniform surface. Twelve glass marbles were placed in a regular pattern on the surface, about 4 cm apart from each other. The animals were placed in the cage and left for 30 min and the number of marbles totally or partially buried (2/3) quantified (Deacon, 2006). The test was performed at 60 and 90 days after challenging either with hRSV, UV-hRSV or mock.

2.6. Open field test

The open field (OF) test measures exploratory and anxious behavior (Carter et al., 2015). This test consists of an open rectangular field box of 460 × 570 × 350 mm. Each animal was placed inside the box for 5 min. In order to evaluate the exploratory behavior at the central area or at the peripheral box, 9 subdivisions were made in the box. The time that each mouse spent at the peripheral or at the central area of the box was recorded. The distance traveled for the mouse in the field was calculated manually by using the measurements from the videos and then scaled to the experimental determinations. The analysis is based on the fact that mice will naturally prefer to be near to the walls and avoid unprotected central area (Carter et al., 2015; Seibenhener and Wooten, 2015). After each trial, the test chambers were cleaned with 70% alcohol and feces were quantified per animal. The test was performed at 60 days after hRSV- or mock- treated.

2.7. Evans blue assay

To evaluate the blood–brain barrier (BBB), mock, UV-hRSV –treated, and hRSV-infected mice were injected intravenously with 2% Evans Blue in PBS after 3- and 7-days post-infection. Then mice were terminally anesthetized with a dose of ketamine/xylazine (100 mg/kg and 20 mg/kg, respectively) 1 h after this injection, transcardiac perfusion was performed with 100 ml of ice-cold PBS, to remove the intravascular dye. Brains and meninges were removed and photographed, then homogenized in 1 ml of 50% trichloroacetic acid, and centrifuged at 10,000 × *g* for 20 min. Samples were quantified at 605 nm in a spectrophotometer and calculations were based on external standards (50–1000 μg/ml) dissolved in the same solvent. The level of Evans blue extravasation was quantified as microgram per gram of brain.

2.8. Sample collection

Mice were terminally anesthetized with a dose of ketamine/xylazine (100 mg/kg and 20 mg/kg, respectively) at 1, 3, 7, 9, 60 and 90 days p.i. Blood from cardiac puncture was obtained to measure cytokine levels in the serum. The bronchoalveolar lavage fluid (BALF) was obtained by injecting 2 ml PBS into the lungs through the trachea. After obtaining the BALF samples, the animals were intracardially perfused with 20 ml of PBS. After perfusion, lung and brain samples were collected for RNA and protein analyses by using RT-qPCR and ELISA, respectively.

2.9. Mouse astrocytes primary cultures and hRSV infection in vitro

Glial primary cultures were performed using a modification of Schildge *et al.,* protocol (Schildge et al., 2013). Briefly, T75 flasks were first coated with 20 ml of a 50 μg/ml poly-D-lysine (PDL) solution in cell culture grade water for 1 h at 37 °C in a CO_2 incubator. At day one to three after birth, animals were euthanized by decapitation using scissors and the brains were obtained and placed into a first dissecting dish filled with Hank's *Balanced Salt Solution* (HBSS). Using a stereomicroscope, the olfactory bulb and cerebellum were removed. Carefully, meninges and hippocampus were dissected. Cortexes were cut into small pieces and transferred to a 50 ml tube with 15 ml of HBSS plus 1.5 ml of 2.5% trypsin and incubated in a water bath at 37 °C for 30 min. The cortex was centrifuged 300xg for 5 min, and the supernatant was discarded. The pellet was dissociated in a single cell suspension in 10 ml of DMEM supplemented with 20% Horse Serum (HS) by pipetting up and down 20 to 30 times. The flasks were washed with sterile water, and the glial cells were plated and incubated at 37 °C at 5% CO_2. After 14 days, microglial cells were separated from astrocytes by shaking at 200 rpm for 1 h at 37 °C. The astrocytes were washed two times with sterile 1X PBS and then incubated with 5 ml of trypsin-EDTA for 10 min at 37 °C. Once astrocytes were detached, 5 ml of DMEM were added to collect the cells and transferred to a 50 ml centrifuge tube. Cells were centrifuged at 180xg for 5 min and the obtained pellet was resuspended in DMEM and plated in a T75 flask. Importantly, in both cases, only astrocytes that are immature grow in culture and once they get confluent and make cell contact, they begin to show a mature phenotype (Lange et al., 2012). *In vitro,* hRSV infection was performed by the exposure of mouse astrocytes to hRSV (MOI: 5) for 2 h at 37 °C in DMEM 1% FBS medium. After incubation, cells were washed 3 times with PBS and incubated in fresh DMEM 1% FBS. After 2, 6, 12, 24, 48 and 72 h, mice cells were collected, and the supernatants were stored at -80 °C for determination of NO levels (see below).

2.10. Quantitative Real-Time qPCR

Total RNA was isolated from lungs and brains using TRIZOL reagent according to the instructions provided by the manufacturer. One microgram of total RNA was reverse transcribed into cDNA using random primers with the iScript cDNA Synthesis kit. Viral loads were evaluated by RT-qPCR in the lungs and brain. Cytokines, chemokines and immunomodulatory molecules were evaluated in the brain. Primers used are detailed in Supplementary Table 1. Quantitative RT-qPCR (SYBR Fast qPCR Master Mix), was carried out in a StepOnePlus™ thermocycler. Relative gene expression data analyses were performed using the comparative $2\Delta^{ct}$ (Pfaffl, 20001). Standard curves for qPCR were generated using pTOPO-N-hRSV or pTOPO-β-actin as templates. The cycle threshold results were entered in the standard curve with the quantity log. Data were expressed as the number of hRSV nucleoprotein transcript copies for each 5 × 10^3 copies of the β-actin.

2.11. Tissue immunofluorescence assays and histology

BALB/cJ mice were terminally anesthetized i.p., with a mixture of ketamine and xylazine (100 mg/kg and 20 mg/kg, respectively) and perfused with PBS at 3 days p.i. Brains for immunofluorescence assays were obtained and covered with the Optimal Cutting Temperature (OCT) compound. The tissue was frozen in cold isopentane and liquid nitrogen for 2 min. Tissue sections were obtained using a Leica cryostat. Brain coronal slides of 30 μm thickness were obtained and the sections were fixed and permeabilized in 70% v/v ethanol for 20 min at −20 °C. Tissue sections were transferred to 100% ethanol for 30 min and dried for another 30 min at RT. Next, tissue sections were hydrated by incubating in 95% ethanol for 30 min, followed by 75% ethanol for 5 min, then to 0.4% Triton X-100 in PBS for 5 min and finally rinsed twice in PBS for 5 min. Sections were incubated in blocking solution (5 mM EDTA, 1% fish gelatin, 2% horse serum, and 1% mostly immunoglobulin free BSA) for 1 h at RT. After that, the sections were incubated with primary antibody overnight at 4 °C at the following concentrations: α -F hRSV (20 μg/ml); and α -GFAP (10 μg/ml) ; MAP-2

(10 μg/ml); vWF (10 μg/ml); Iba-1 (6 μg/ml), and the antibodies were diluted in blocking solution. Fixed sections were washed four times with PBS for 5 min and incubated with polyclonal goat α -mouse conjugated to Alexa Fluor 488 (10 μg/ml) and polyclonal goat α -rabbit Alexa Fluor 555 (10 μg/ml) for 1 h at RT, followed by 4 washes in PBS for 5 min. Nuclei were stained with DAPI (1 μM) for 10 min. Coverslips were mounted and examined in a Fluoview FV1000 Laser Scanning Confocal Microscope (Olympus, Melville, NY). Images were processed using FV10-ASW 1.7 software (Olympus) and the confocal microscopy settings were adjusted using the fluorescence derived from the secondary antibody to minimize the brain autofluorescence. Quantification of immunofluorescence images was performed using Image J software (Schneider et al., 2012).

2.12. Flow cytometry

Flow cytometry was used to measure neutrophils infiltration in Bronchoalveolar lavage fluid (BALF) as a means to quantify pulmonary disease in challenged animals. BALF was obtained using 1X PBS, and lungs were collected after perfusion with 20 ml of PBS 1X. Lung samples were homogenized and filtered using 40-mm cell strainers. BALF and lung cellular suspensions were centrifuged at 300xg for 5 min, washed and stained with α-CD45 PE, α-CD11b PE-Cy7, α-Ly6G FITC and α-CD11c APC (Clone HL3, BD Pharmingen) for 45 min at 4 °C. Data acquisition was performed on a FACS Canto-II flow cytometer (BD Biosciences) and analyzed using FlowJo 7.6 software. Absolute quantification of cell numbers was conducted using CountBright™ Absolute Counting Beads. Beads were added in a dilution 1/30 to each BALF samples. To evaluate the infiltrating cells into the CNS, brains from perfused animals were collected, and mononuclear cell suspensions were isolated from brain tissue as follows. Brain tissue was digested using type IV collagenase (1 mg/ml) and DNase I (50 μg/ml) for 30 min at 37 °C. Brain samples were homogenized and filtered using a 40 μm pore cell strainer. The homogenate was centrifuged at 200xg for 10 min at 4 °C. The pellet was resuspended in 5 ml of 70% isotonic Percoll and loaded in a tube containing 30% isotonic Percoll. The Percoll gradient was centrifuged at 700xg for 20 min at 4 °C. Mononuclear cells were collected from the interface 70/30%, washed and stained with α-CD45 PE, α-CD11b PE-Cy7, α-Ly6G FITC, α -Ly6C-PercCP 5.5, α- B220 APC Cy7, α- CD19 PE-Cy7, α- CD4 APC and α- CD8 FITC. Data acquisition was performed on a FACS Canto-II flow cytometer (BD Biosciences) and analyzed using FlowJo 7.6 software. The gate strategy for this analysis is shown in Supplementary Fig. 1.

To evaluate the hRSV infection and GFAP expression in murine astrocytes primary culture, cells were harvested at 24, 48 and 72 h p.i. Then, cells were fixed with 2% PFA-PBS for 15 min at RT and permeabilized with saponin 0,05% in PBS for 20 min at RT, washed and stained with α-GFAP eFluor® 660 and α-F-hRSV (Palivizumab) Alexa 488 (0.3 μg/ml and 20 μg/ml respectively). Data acquisition was performed on a FACS Canto-II flow cytometer and analyzed using FlowJo 7.6 software. Supplementary Fig. 5 shows a scatter- graph for the gating strategy and a histogram depicting the number of cells positive for GFAP staining.

2.13. Enzyme-linked immunofluorescence assay (ELISA)

Serum samples were directly used for quantification of TNF-α, IL-6, IL-4 by ELISA kit (BD OptEIA™, BD Biosciences Pharmingen, San Diego, CA), and CCL2 (R&D System), with a technique sensitivity approximately equal to 2–4 pg/ml. Brains were used for quantification of TNF-α, IL-6, IL-10, IL-4, GFAP, CD200, and CCL2. Each sample was previously homogenized in RIPA buffer (Tris-HCl: 50 mM, pH 7.4, Nonidet P-40: 1%, Na-deoxycholate: 0.5%, SDS 0.1% EDTA: 0.5 mM, Protease Inhibitor Cocktail: 500 μM AEBSF, HCl, 150 nM Aprotinin, 1 μM E-64, 0.5 mM EDTA, Disodium Salt and 1 μM Leupeptin Hemisulfate). Then for each sample, total protein was quantified by the BCA method and 500 μg of total proteins were used for the ELISA following the protocol suggested by the manufacturer.

2.14. Quantification of NO production

NO production by mouse astrocytes primary cultures was determined by measuring nitrite (NO^{-2}) using the Griess assay method as previously described (Flores and von Bernhardi, 2012). NO^{-2} is a stable metabolite derived form NO that correlates well with NO production (Flores and von Bernhardi, 2012; Brahmachari et al., 2006; Buskila et al., 2005). Briefly, mouse astrocytes primary cultures were infected with hRSV at MOI equal to 5. Supernatants were collected after 2, 6, 12, 24, 48 and 72 h p.i. An aliquot of 50 μl was mixed with a solution of 10 μl of 0.5 M EDTA/H_2O (1:1), pH 8.0, and 60 μl of freshly prepared Griess reactive. A calibration curve was established by using solutions of 5 to 80 μM $NaNO_2$ as a standard. The production of NO^{-2} was measured by absorbance at 540 nm by using an automated ELISA reader (EPOCH, Biotek).

2.15. Statistical analyses

All statistical analyses were performed using Prism 6.1 Software for Windows. Statistical significance was evaluated by one-way ANOVA (Kruskal-Wallis test) and/or two-way test with Bonferroni or Tukeý́s post-test, and Area Under the Curve (AUC). Differences were considered significant with a $p\text{-value} < 0.05$. Mann-Whitney U test or unpaired t-test was used to compare two groups at the same time point. A p-value **** $P < 0.0001$, *** $P < 0.0005$, ** $P < 0.005$, * $P < 0.05$, was considered significant.

3. Results

3.1. hRSV induces disease in mice and viral RNA is detected in both, lungs and brain tissue

Disease progression of mice infected with hRSV or UV-hRSV and mock-treated mice were monitored by measuring the body weight of infected mice. As expected, hRSV-infected mice displayed significant weight loss at day 2, 3 and 4 p.i. as compared to mock-treated and UV-hRSV challenged animals (Fig. 1A). Airway inflammation was also measured by performing flow cytometry on the bronchoalveolar lavage fluids (BALFs). Consistent with the findings described above we observed an increase in the percentages of neutrophils in the BALFs of hRSV-infected mice (40%) as compared to UV-hRSV and mock-treated animals (18%) (Fig. 1B). Additionally, viral loads were quantified by measuring N-hRSV (nucleoprotein N gene of hRSV) mRNA levels in the lungs and brains of treated mice. As expected, N-hRSV mRNA peaked at 7 days p.i. in the lungs and at 3 days p.i. in the brains of hRSV-infected mice (Fig. 1C and 1D). It is noteworthy to mention that infectious hRSV particles (PFUs) could not be recovered from the brains of infected mice, likely due to low viral loads in this organ, as compared to the lung tissue. These data are in agreement with our previous report assessing infection with the viral isolate 13018-8 obtained from a local clinic (Obodai, 2018). We had previously published that the highest loads of hRSV were observed at day 7 and day 3 p.i. at the lungs and brain respectively (Espinoza et al., 2013).

3.2. hRSV infection alters the digging and exploratory behavior in mice post-challenge

Previously, we reported that after 30 days post-infection with hRSV mice showed alterations at the hippocampal function demonstrated as reduced spatial memory and poor digging behavior (Espinoza et al., 2013). In this study we evaluated whether the digging, which is a repetitive behavior that depends on ventral hippocampal function, was impaired in mice up to 60- and 90-days post-infection with hRSV.

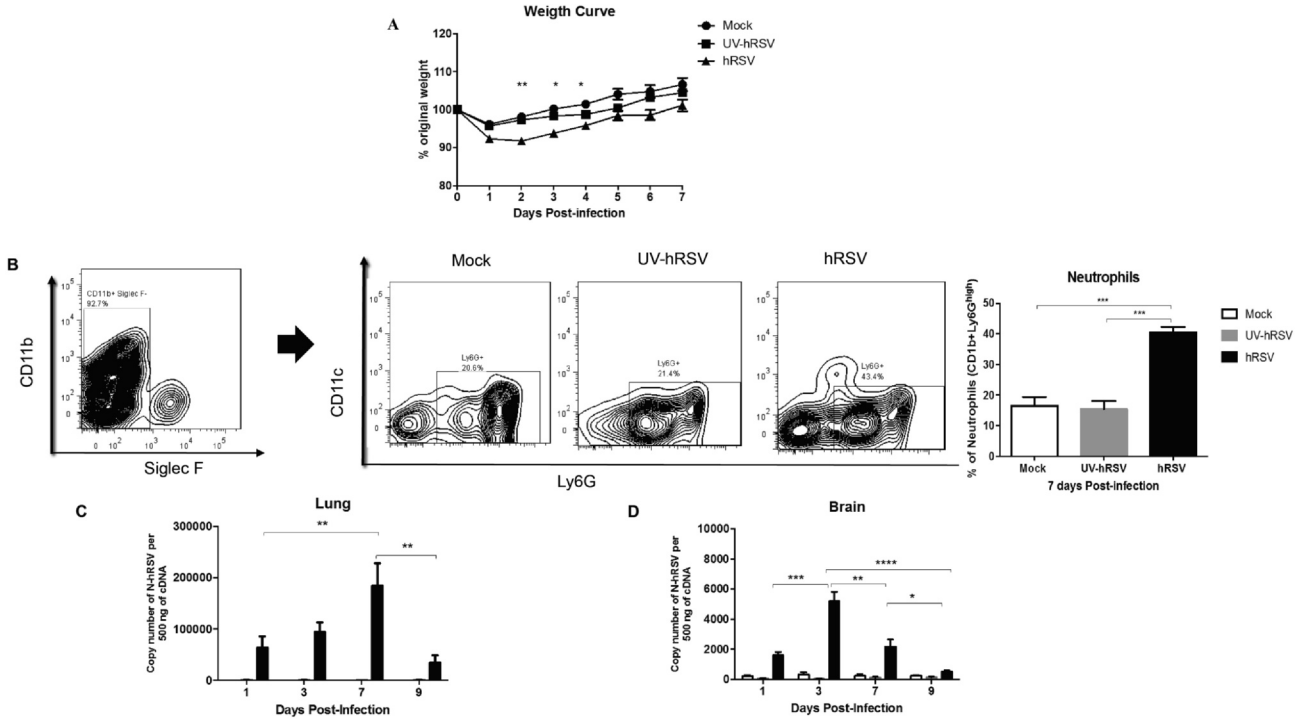

Fig. 1. hRSV infection in mice. **(a)** This graph shows body weight data during 7 days for mice that were intranasally infected with 1x10^6 PFU of hRSV or UV-hRSV, or mock-treated. The results combine data from three independent experiments performed (N = 3 mice per experimental group per each experiment). Comparisons between groups were made using one-way ANOVA test with Tukeýs post-test, ** P < 0.01, *P < 0.05. Bars represent mean ± SEM. BALF was harvested 7 days pi. **(b)** Contour plots show the gating strategy to select the CD11b$^+$ Siglec F$^-$ cell population. Representative BALF contour plots of mock-treated and hRSV-infected mice. Neutrophils were characterized as the CD11b$^+$ Siglec F$^-$ CD11c$^-$ Ly6G^{high} cell population. One-way ANOVA test with Tukeýs post-test, * P < 0.05. Graphs show the quantification of N-hRSV mRNA in the lungs **(c)** and in the brain **(d)** of mice after mock (white bar) or UV-hRSV (gray bar) treatment or hRSV infection (black bar). Three independent experiments were performed (N = 3–4 mice per experimental group per each experiment). Comparisons between groups were made with the Kruskal-Wallis *U* test, **** P < 0.0001, *** P < 0.001, ** P < 0.01, * P < 0.05. Bars represent mean ± SEM.

Fig. 2A and 2B show representative images of MB tests performed at 60- or 90-days p.i., respectively. A significant impairment in the digging behavior was detected after 60 days p.i. in hRSV-infected mice as compared to UV-hRSV- and mock-treated mice (Fig. 2C). However, 90 days p.i. hRSV-infected mice showed a normal digging behavior suggesting that this alteration in mice endures long but it recovers (Fig. 2B and D). Mice after 60 days p.i. with hRSV showed an enhanced exploratory behavior in the open field test at the central area of the box compared to the peripheral area (Supplementary Fig. 2).

3.3. High levels of IL-4, IL-10 and GFAP mRNA and protein are detected in the CNS of mice after 60 days of post-infection with hRSV.

It has been previously shown that cytokines, such as IL-6, TNF-α, IL-1β, IL-4, IL-10, and CD200 can affect the behavior, learning and memory of animals (Avital et al., 2003; Balschun et al., 2004; Santello and Volterra, 2012; McAfoose and Baune, 2009; Pozner, 2008; Donzis and Tronson, 2014). Moreover, the high expression of GFAP by astrocytes has been related to astrocyte activation, inflammation and neurodegenerative diseases (Anderson et al., 2014; Brenner, 2014; Middeldorp and Hol, 2011). We think that it is possible that the content of these cytokines and GFAP could be altered in the brain of mice infected with hRSV. Therefore, the mRNA levels of IL-6, TNF-α, IL-1β, IL-4, IL-10, CD200 and GFAP were analyzed in the brains from hRSV-infected mice 60 days p.i. Similar levels of IL-6, TNF-α, CX3CL1, IL-1β and CD200 mRNAs were observed in the brains of hRSV-infected mice as compared to mock- and UV-hRSV-treated mice (Fig. 3A). Interestingly, 60 days p.i. a significant increase was observed for IL-4, IL-10, CCL2 and GFAP mRNA levels in hRSV-infected mice. The expression of TNF-α mRNA and protein content were similar among all experimental groups (Fig. 3A and 3B, respectively). A significant increase in the protein content of IL-4 (Fig. 3C) and IL-10 (Fig. 3D) and GFAP (Fig. 3E) was observed in hRSV-infected mice as compared to UV-hRSV- and mock-treated mice. The protein levels of these molecules were consistent with their mRNA levels.

3.4. Increased blood–brain barrier permeability and immune cell infiltration into the brains of hRSV-infected mice

It has been observed an increase in the BBB permeability in mice infected with influenza virus (Hosseini et al., 2018). Given that and that we previously were able to identify hRSV in the brain cortex (Espinoza et al., 2013) at 3 days p.i., here we evaluated whether the hRSV infection promotes an alteration of the BBB permeability and inflammatory cell infiltration. For that BALB/c mice were either intranasally (i.n.) infected with 1x10^6 PFUs of hRSV or inoculated with non-infectious supernatant (i.e., mock) or UV-inactivated hRSV. After 3 or 7 days of infection BBB permeability was measured by Evans blue extravasation into the brain (see materials and methods). Evans blue is a cationic dye that binds to albumin in the serum and forms a complex that under normal conditions is not able to trespass an intact BBB (Varatharaj and Galea, 2017). Thus, extravasation of the Evans blue-albumin complex into the brain is indicative of increased BBB permeability to macromolecules (Roe et al., 2012). Mock- or UV-hRSV treated mice showed no significant extravasation of Evans blue into the brain (Fig. 4A and B). However, hRSV-infected mice showed a significantly increase of Evans blue extravasation into the brain at 3 days p.i. (Fig. 4A and 4C). Even though, after seven days p.i. the amount of Evans Blue detected at the CNS was reduced (Fig. 4B and 4D), it was significantly high, suggesting that the permeability of the BBB to macromolecules was increased in hRSV-infected mice.

Moreover, it is possible that not only the BBB permeability was

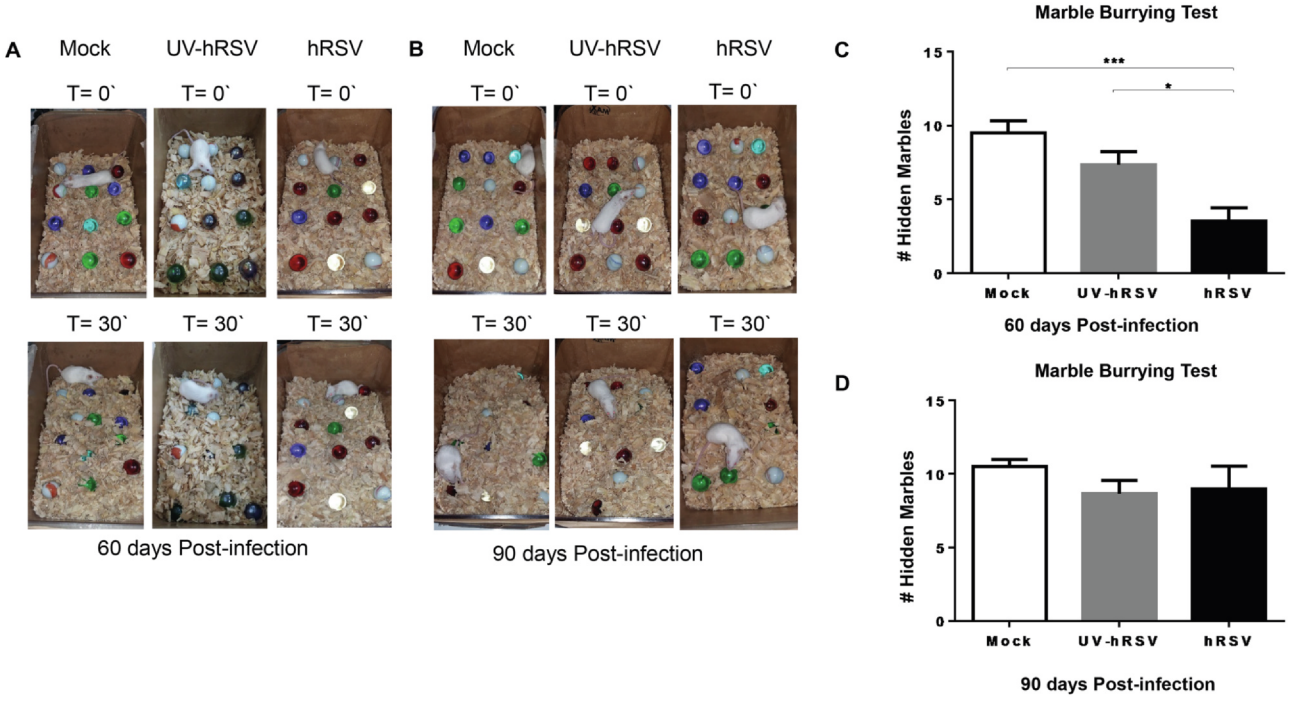

Fig. 2. Mouse digging behavior remains impaired for up to 60 days after hRSV infection. Mice were intranasally infected with $1x10^6$ PFU of hRSV or UV-hRSV, or mock-treated and then MB-tested 60 and 90 days p.i. Upper panels show the initial position of marbles and the lower panels show marbles position after 30 min (*T = 30′*). **(a)** Representative photographs of the MB test performed after 60 days. Two independent experiments were performed (N = 2–3 mice per experimental group per each experiment) and **(b)** 90 days (N = 2 mice per group per experiment) p.i. with hRSV. **(c)** The graph shows the quantification of the number of hidden marbles at 60 days and **(d)** at 90 days p.i. Mann-Whitney *U* test. *** P < 0.0005, *P < 0.05 indicates that means are significantly different. Bars represent mean ± SEM. (For interpretation of the references to colour in this figure legend, the reader is referred to the web version of this article.)

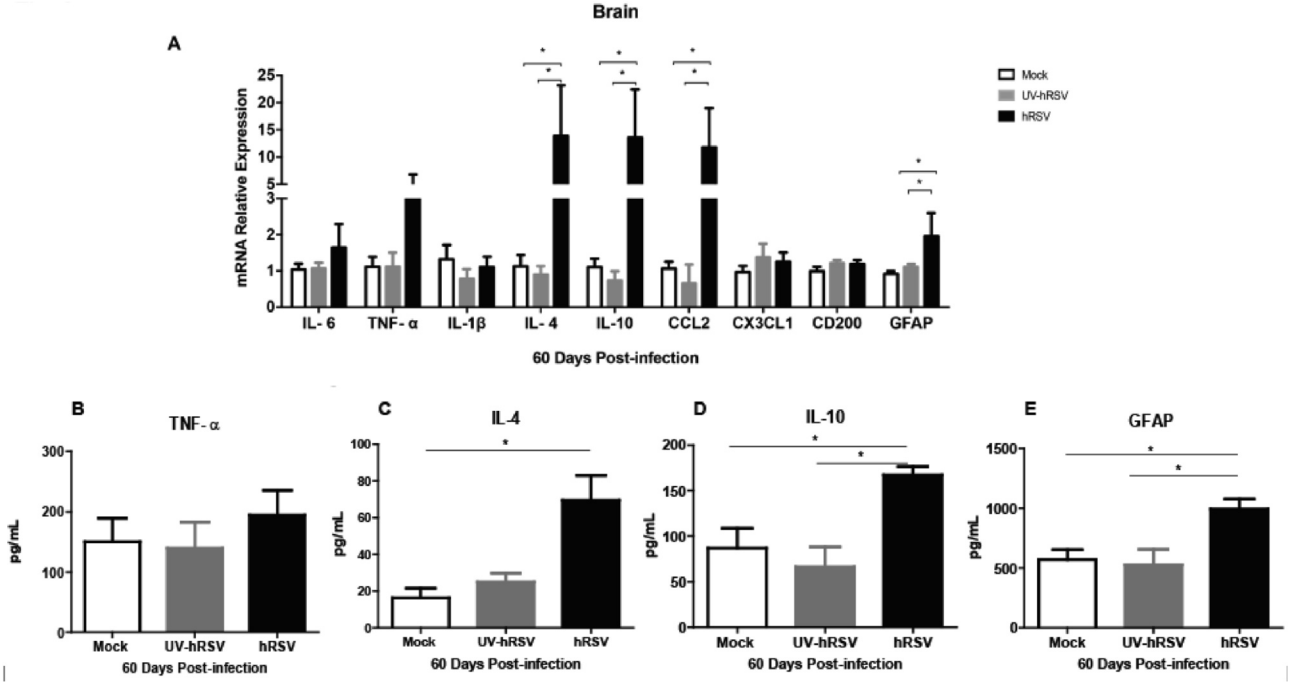

Fig. 3. Expression of GFAP and molecules that contribute to inflammation were increased in the brains of mice at 60 days post-infection with hRSV. mRNA and protein expression of GFAP and immunomodulatory molecules were analyzed in the brains of mice that were intranasally infected with $1x10^6$ PFU of hRSV or UV-hRSV-treated for 60 days and after performing the MB test **(a)** The graph shows mRNA relative expression for IL-6, IL-1β, CD200, GFAP, TNF-α, IL-4, IL-10, CCL2 and CX3CL1 using β-actin as a housekeeping control gene. Graphs show the quantification of TNF-α **(b),** IL-4 **(c)**, IL-10 **(d)** and GFAP **(e)** by ELISA from the brains of these mice. Two independent experiments were performed (N = 2–3 mice per experimental group per each experiment). Comparisons between groups were done using one-way ANOVA test with Tukeýs posttest. *P < 0.05 indicates means are significantly different. Bars indicate mean ± SEM.

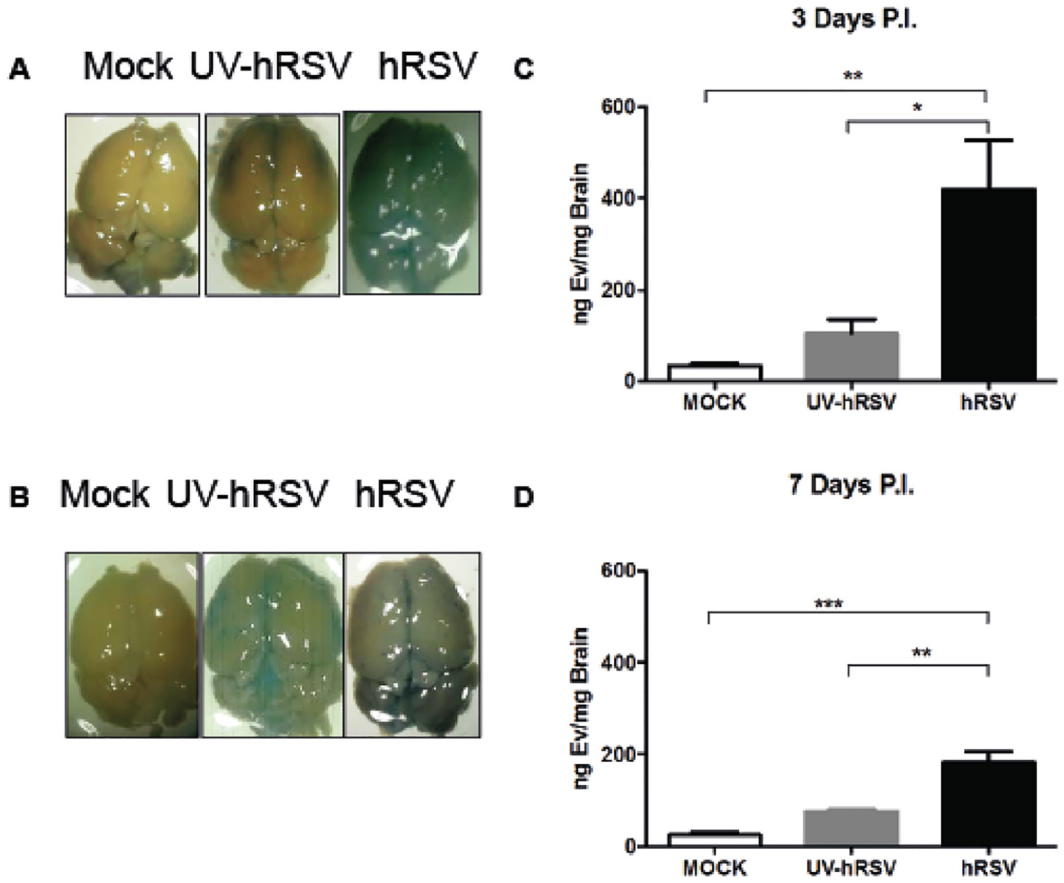

Fig. 4. hRSV infection induces BBB permeability *in vivo*. Mice that were intranasally challenged with $1x10^6$ PFU of hRSV or UV-hRSV, or mock-treated and the permeability of the BBB was measured using Evans blue dye at day 3 and 7 p.i. (**a**) Representative images of the brain of mice for each treatment and the quantification of Evans blue dye in the brain of infected mice at 3 days p.i. (**b**) Representative images of the brain of mice for each treatment and the quantification of Evans blue dye in the brains of infected mice at 7 days p.i. Three independent experiments were performed (N = 9 mice per group for each experiment). Comparisons between groups were made with one-way ANOVA test with Tukeýs post-test. ** P < 0.005, *P < 0.05 indicate that means show significant statistical differences. Bars indicate mean ± SEM. (For interpretation of the references to colour in this figure legend, the reader is referred to the web version of this article.)

increased to macromolecules but also the infiltration of inflammatory cells into the CNS. We assessed the presence of inflammatory cells into the brain parenchyma of hRSV-infected mice. Immune cell infiltration was evaluated by flow cytometry at days 3 and 7 p.i. with hRSV, UV-hRSV or mock treatments (Fig. 5). A significant increase in neutrophils (Fig. 5A and 5D), and inflammatory monocytes (Fig. 5A and 5F) was observed in the brains of hRSV-infected mice 3 days p.i. when compared to UV-hRSV-challenged or mock-treated mice. Resident macrophages cells were also analyzed (Fig. 5A and 5E) and a significant increase in hRSV-infected mice was only observed when compared to mock-treated mice. As microglia expresses similar surface markers as macrophages, we used the Ly6C marker because it had been previously described that microglial cells do not express this surface protein (Greter et al., 2015). At 7 days p.i., no significant differences were found. The population of $CD4^+$ T cells was similar in the brains of all experimental groups after 3 or 7 days p.i. (Fig. 5C and 5H). On the other hand, a significant infiltration of $CD8^+$ T cells (Fig. 5C and 5I) and B cells (Fig. 5B and 5G) was observed at 7 days p.i. in the brains of hRSV-infected mice as compared to UV-hRSV- or mock-treated mice.

3.5. hRSV infection induces the expression of pro-inflammatory cytokines and immunomodulatory molecules in the brain of infected mice.

Given the observation that immune cell populations were increased in the brains of hRSV-infected mice, selected inflammatory cytokines were analyzed in the brains of mock-treated, as well as UV-hRSV- and hRSV-infected mice by qPCR and ELISA (Fig. 6). To corroborate the data dispersion an area under the curve (AUC) analysis was performed (Supplementary Fig. 4). IL-6 mRNA expression was increased at day 1 and 7 p.i. in the brains of hRSV-infected mice, as compared to UV-hRSV- and mock-treated mice (Fig. 6A). Consistently, the amount of IL-6 protein found in the brains of hRSV-infected mice was significantly increased at day 3 and 7 p.i. as compared to UV-hRSV- and mock-treated mice controls (Fig. 6F). A lack of a significant increase in the serum levels for IL-6 after hRSV infection suggested that the increase of this cytokine was localized in the CNS and not a systemic phenomenon due to viral infection (Supplementary Fig. 3A). A significant decrease of TNF-α mRNA was detected at day 9 p.i. for hRSV-infected as compared to UV-hRSV- and mock-treated mice (Fig. 6B). In contrast, a significant increase of TNF-α protein levels were detected at day 1 p.i. in hRSV-infected mice, as compared to mock-treated animals and at day 3 p.i. in hRSV-infected mice, as compared to UV-hRSV-treated and mock-treated animals (Fig. 6G). The serum levels of TNF-α were similar in all experimental groups at any time-point(Supplementary Fig. 3B). A significant increase in IL-4 mRNA was observed in the CNS of hRSV-infected mice at days 1 and 3 p.i. as compared to UV-hRSV- and mock-treated mice (Fig. 6C). Consistently, a significant increase in IL-4 protein was detected at days 1, 7 and 9 p.i. as compared to mock-treated mice. (Fig. 6H). As expected, no significant differences in serum levels were observed for IL-4 among hRSV-, UV-hRSV- or mock-treated mice (Supplementary Fig. 3C).

The level of CCL2 was analyzed in the brains of hRSV-infected mice because this molecule it is a potent chemoattractant for monocyte (Deshmane et al., 2009). Consistently, there was a higher number of

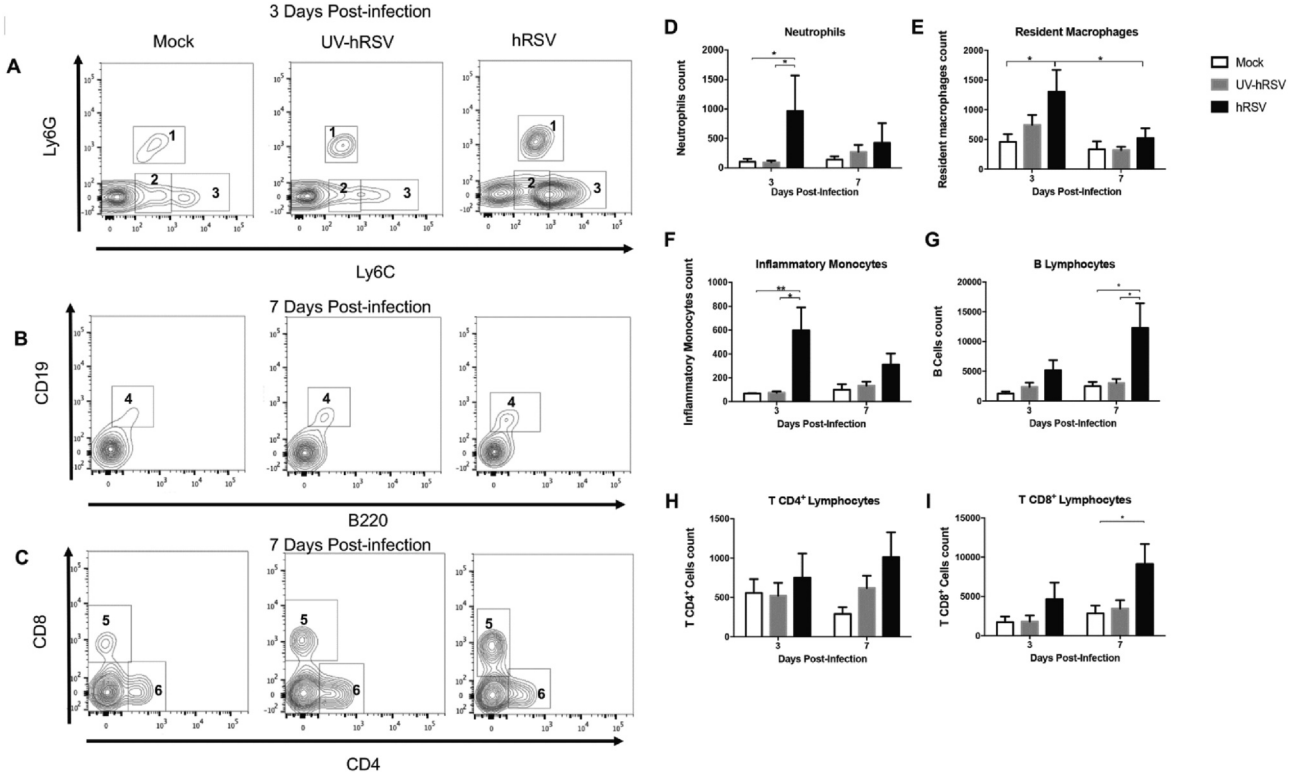

Fig. 5. Immune cell infiltration into the CNS of hRSV-infected mice. Immune cell infiltration in the brain of mice that were intranasally infected with $1x10^6$ PFU of hRSV or UV-hRSV and mock-treated mice were analyzed by flow cytometry. **(a-c)** Representative contour plot for the analyzed immune cells (1: Neutrophils, 2: Resident macrophages, 3: Inflammatory monocytes, 4: B cells, 5: $CD8^+$ T cells, and 6: $CD4^+$ T cells). The graph shows the number of **(d)** neutrophils, **(e)** resident macrophages, **(f)** inflammatory monocytes **(j)** B cells, **(h)** $CD4^+$ T cells, and **(i)** $CD8^+$ T cells in the brain of hRSV-infected mice, UV-hRSV infected mice and mock-treated mice 3 and 7 days post-infection. Two independent experiments were performed (N = 3–4 mice per group per each experiment). Comparisons between groups were done using one-way ANOVA test with Tukeýs post-test. *P < 0.05 indicates that means are significantly different. Bars indicate mean ± SEM.

inflammatory monocytes in the brains of hRSV-infected mice (Fig. 5F). An increase in CCL2 mRNA and protein levels was observed at day 3 p.i. (Fig. 6D, 6I). No significant differences were observed when CCL2 was measured in the serum of hRSV-infected mice as compared to mock controls. A decreasing trend was observed over time in infected animals (Supplementary Fig. 3D).

In the CNS, microglia and astrocytes are the most abundant cells (Moriguchi et al., 2020); these cells contribute to the regulation of the immune response at the CNS (Bernard-Valnet, 2020). In the brain, CD200 is a type-1 membrane glycoprotein expressed by neurons,

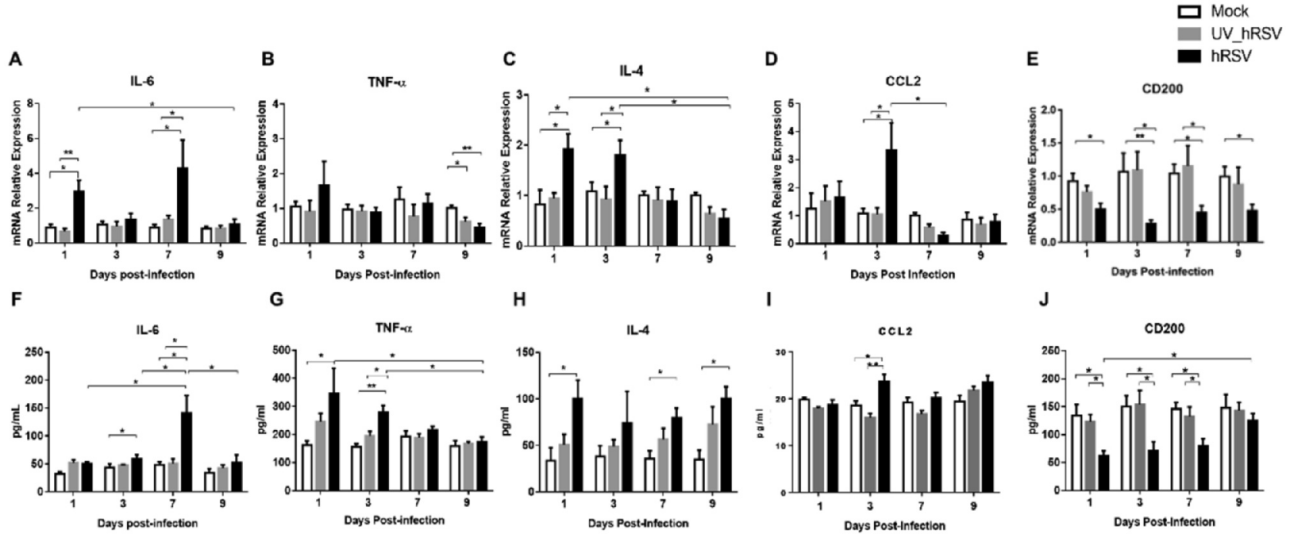

Fig. 6. Increased expression of inflammatory cytokines in the CNS of hRSV-infected mice. mRNA and protein levels of cytokines (analyzed by RT-qPCR and ELISA) in the brain of mice intranasally infected with $1x10^6$ PFU of hRSV or UV-hRSV and mock-treated mice. The following graphs show mRNA levels for: **(a)** IL-6; **(b)** TNF-α; **(c)** IL-4**; (d)** CCL2; and **(e)** CD200. The following graphs show the content of protein levels for: **(f)** IL-6; **(g)** TNF-α; **(h)** IL-4; **(i)** CCL2; and **(j)** CD200. Three independent experiments were performed (N = 3–4 mice per experimental group per each experiment). Comparisons between the groups were done using one-way ANOVA test with Tukeýs posttest. ** P < 0.005, *P < 0.05 indicates means are significantly. Bars indicate mean ± SEM.

oligodendrocytes, and reactive astrocytes. Importantly, CD200 is an immunosuppressive molecule (Rogers et al., 2020) and its interaction with its receptor, (CD200R) which expressed by the microglia, modulates microglia activation (Rogers et al., 2020). During inflammatory conditions, the downregulation of CD200 leads to increased activation of microglia (Rogers et al., 2020). Moreover, it has been observed that the downregulation of CD200 leads to cognitive impairment (Hornuss, 2020). Thus, the levels of CD200 mRNA and protein were measured in the brains of hRSV-infected mice. As shown in Fig. 6E a significant decrease in CD200 expression was observed at days 1, 3, 7 and 9 p.i. in hRSV-infected mice, as compared to UV-hRSV- and mock-treated mice. Similar results were obtained when protein levels of CD200 were quantified showing significant differences at days 1, 3, 7 p.i. (Fig. 6J).

Another molecule with important immunomodulatory effects in the CNS is the chemokine CX3CL1, which exists both as membrane-bound and soluble forms (Jones et al., 2010). The chemokine CX3CL1 is expressed by neurons and its receptor CX3XR1 is expressed by microglia (Bertollini et al., 2006; Hansen, 2001; Lauro et al., 2015). Importantly, the CX3CL1- CX3CR1 axis keeps microglia in a resting state and the loss of CX3CL1 expression promotes the activation of microglial cells (Lauro et al., 2015; Ransohoff and Cardona, 2010). Interestingly, a significant decrease in CX3CL1 mRNA expression was found at day 3 p.i. in the brains of hRSV-infected mice, as compared to UV-hRSV- and mock-treated mice (Supplementary Fig. 3E).

Additionally, it has been described that hRSV infection impairs the antiviral activity of IFN-α and IFN-β in the infected host (Spann et al., 2004). Mice infected with other respiratory viruses, such as influenza have shown alterations in the expression of type-I IFNs (IFN-α and IFN-β) in the brains that could be associated with a cognitive impairment (Jurgens et al., 2012). When the expression of IFN-α and IFN-β was measured in the brains of hRSV-infected mice, a significant increase was detected for IFN-α and IFN-β at day 1 p.i. and at 7 days p.i., respectively (Supplementary Fig. 3F and G). A significant decrease in the expression of IFN-α and IFN-β mRNAs was detected at day 3p.i. (Supplementary Fig. 3F and 3G).

3.6. CNS cells can be infected by hRSV in vivo

It has been previously proposed that hRSV can reach the brain at 3 days p.i. (Espinoza et al., 2013) and it enters into the CNS utilizing a *"Trojan horse"* mechanism (Miner and Diamond, 2016). However, whether hRSV can infect and replicate in cells of the CNS remains unknown. Therefore, we evaluated whether hRSV could infect astrocytes, neurons, microglia and endothelial cells at day 3 p.i. with 1×10^6 PFUs. Fig. 7 shows representative pictures of immunofluorescence co-localization analyses in brain cortex for hRSV and various markers for CNS cells. F-hRSV colocalized with 1% of endothelial cells (Fig. 7B), 1% of neurons (Fig. 7C) and 1% of microglia (Fig. 7D). Whereas, F-hRSV colocalized with 5% of astrocytes (Fig. 7E). Moreover, we also detected approximately 4% of F-hRSV $^{\pm}$ free, which means that the viral protein was not associated with any of the analyzed cell types. These results suggest that even if all these cell types could show the presence of hRSV antigens, astrocytes were more susceptible to infection by this virus.

3.7. hRSV infection activates astrocytes in vitro

Astrocytes display several immune functions, such as antigen uptake and presentation to T cells, as well as the secretion of cytokines and immunomodulatory molecules (Farina et al., 2007; Dong and Benveniste, 2001). According to this notion and because we found that the percentage of hRSV-infected astrocytes was higher as compared to the other cell types (Fig. 7), the hRSV infection was evaluated by flow cytometry in mouse primary astrocyte cell cultures that were inoculated with a MOI equal to 5. Supplementary Fig. 5 shows a scatter graph for the gating strategy and a histogram depicting the number of cells positive for GFAP staining. To corroborate the data dispersion an area under the curve (AUC) analysis was performed (Supplementary Fig. 6). Importantly, expression of F-hRSV was detected in murine astrocytes cultured *in vitro* and the levels of this protein increased over time, supporting the notion that hRSV can infect these cells (Fig. 8A). Furthermore, quantification of N-hRSV mRNA at various time-points showed an increase at 24 h p.i. and then a reduction after 48 and 72 h p.i. with hRSV (Fig. 8B). Interestingly, the median fluorescence intensity (MFI) of GFAP was quantified in astrocytes and observed an increase over time along with the expression of F-hRSV (Fig. 8C). The observed astrocyte activation upon hRSV infection was consistent with the increase in GFAP content found in these cells (Eng and Ghirnikar, 1994).

To determine whether astrocytes can be activated during hRSV infection, intracellular levels of nitric oxide (NO) were quantified as a marker for astrocyte activation (Pozner, 2008). Importantly, the production of NO increased in hRSV-infected astrocytes 24, 48 and 72 h p.i., as compared to UV-hRSV-treated cells (Fig. 8D). These data further support the notion that hRSV activates astrocytes and that this virus is likely that could induce an inflammatory response in the CNS. Therefore, we also measured the secretion of cytokines associated with inflammation, such as IL-4, IL-10, TNF-α and IL-6 in the supernatants of astrocytes exposed to hRSV. A significant increase in IL-4 was detected after 6 and 12 h p.i. as compared to mock-treated astrocytes (Fig. 8E). A peak in IL-10 secretion was detected at 6 h post hRSV-infection (Fig. 8F). TNF-α also increased in the supernatants of hRSV-infected astrocytes, but 12 h p.i., as compared to control cells (Fig. 8G). Further, IL-6 secretion significantly increased in astrocytes infected with hRSV between, 12 h to 72 h, p.i. as compared to control cells (Fig. 8H). These results suggest that hRSV infection induces an inflammatory response in astrocytes that is mediated by the secretion of molecules with immunomodulatory and inflammatory properties, such as for IL-10, IL-4 and TNF-α and IL-6.

4. Discussion

Neurological complications in patients with severe bronchiolitis due to infection with hRSV have been increasingly reported in the past years (Sweetman et al., 2005; Kawashima et al., 2009; Kawashima et al., 2012; Millichap and Wainwright, 2009; Morichi et al., 2011, 2017). Importantly, viral mRNA has been detected in CSF samples of patients with neurological alterations, suggesting that hRSV can reach the CNS (Eisenhut, 2007, 2006; Morichi et al., 2011; Zlateva and Van Ranst, 2004). Furthermore, an increased cytokine level detected in the CSF of hRSV-infected patients suggests that CNS infection could be accompanied by encephalitis (Bohmwald, 2019; Kawashima et al., 2009, 2012; Millichap and Wainwright, 2009; Otake et al., 2007; Zlateva and Van Ranst, 2004). Consistently these important observations in hRSV-infected patients, in this study we reported that neurological symptoms could also take place in animal models. These data further support the notion that hRSV can access to the CNS, in particular by infecting astrocytes. However, clinical signs associated with the encephalopathy described in humans by hRSV, such as seizures (Morichi et al., 2011, 2017) were not observed in the murine model. Importantly, our findings are in agreement with previous data suggesting that hRSV may enter the CNS by a "*Trojan horse*" mechanism, by infecting monocytes and B cells (Zhivaki et al., 2017; Takeuchi et al., 1998); as well as peripheral blood monocytes (Torres et al., 2010). Indeed, blockade of integrin α_4 with a neutralizing anti-CD49d antibody prevented hRSV entry into the CNS, which supports the idea that cells carrying the virus would require crossing the BBB to access the CNS, but not the lungs (Espinoza et al., 2013; Puntambekar et al., 2011).

This work provides evidence suggesting that even up to 60 days after hRSV infection mice still display a poor repetitive behavior (Fig. 2). Because motor alterations in mice infected with hRSV were previously ruled out (Espinoza et al., 2013); our data suggest that the infection caused a long lasting effect at least over ventral hippocampal

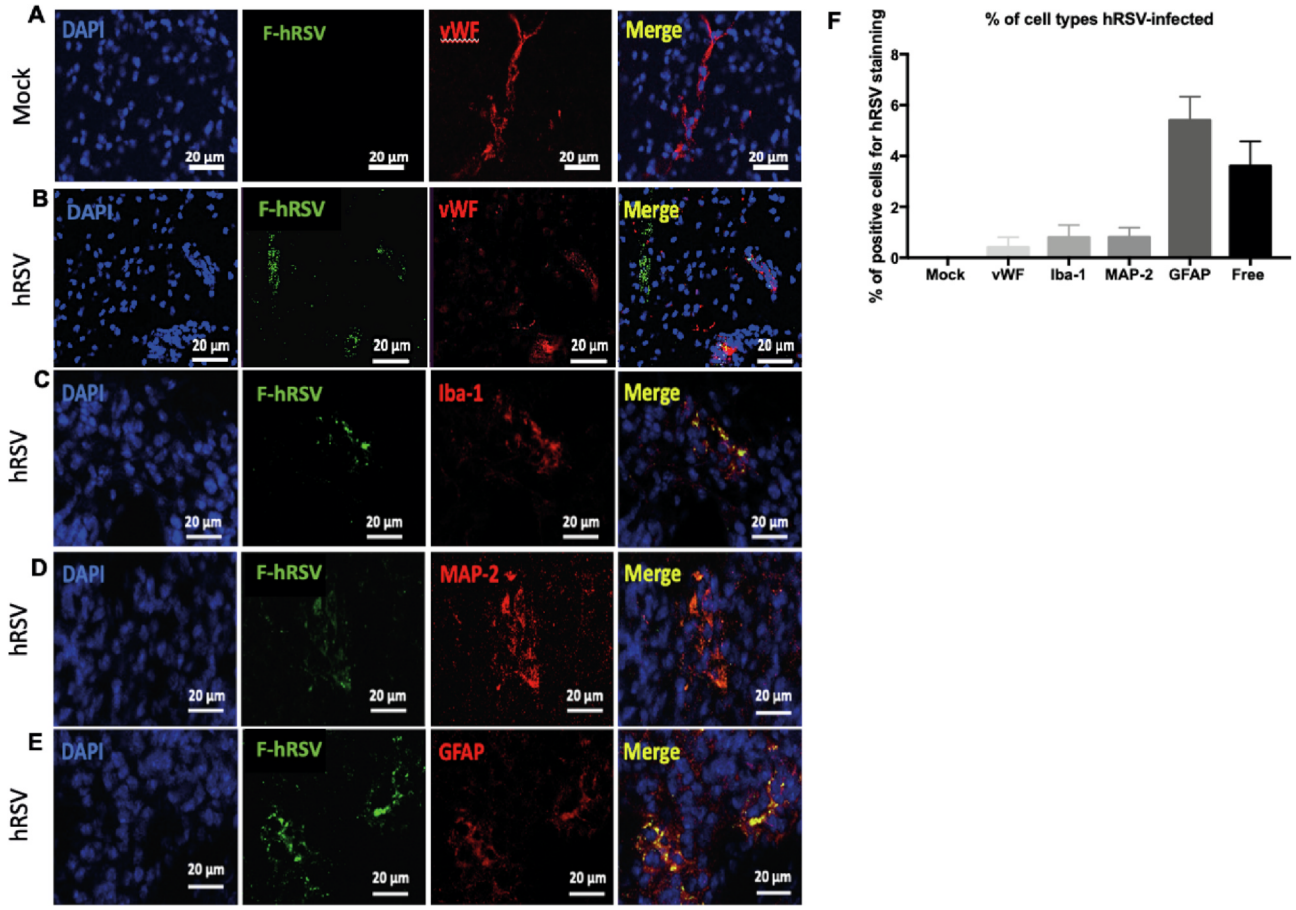

Fig. 7. hRSV infects different CNS cell types *in vivo*. Mice were intranasally infected with $1x10^6$ PFU of hRSV or mock-treated and brains were obtained 3 days p.i. Representative immunofluorescence images of (a) F-hRSV and vWF for mock mice. Representative immunofluorescence images of F-hRSV with **(b)** vWF, **(c)** Iba-1 **(d)** MAP-2 and **(e)** GFAP proteins were analyzed hRSV-infected mice at 20X magnification. The hRSV F-protein is visualized in green, the cell markers in red and cell nuclei in blue. **(f)** The co-localizations of F-hRSV and tprotein markers for each type of cell are visualized in yellow and were quantified to determine the percentage of F-hRSV$^+$ cells in whole field. Two independent experiments were performed (N = 6–7 mice per experimental group per each experiment). Comparisons between groups were performed with Mann-Whitney *U* test. Bars indicate mean ± SEM.

functions (Wang, 2019). The aim of this study was to evaluate only the behavioral long-term alterations after hRSV infection. Therefore, the MB test was chosen for its capacity to assess behavioral alterations in mice including the digging and repetitive behavior (Deacon, 2009; Thomas et al., 2009). To further evaluated the behavioral alterations, an open field test was performed. During this test, it was clearly observed that hRSV-infected mice increased their exploratory behavior and the amount of time spent in the central area, but not at the peripheral area (Supplementary Fig. 2), which is not their common behavior (Carter et al., 2015). No differences were observed in the defecation frequency indicating that both experimental groups displayed similar levels of anxiety (Seibenhener and Wooten, 2015). Despite these observations, it would be needed to perform additional tests in future studies to have a more complete view regarding the alterations to the CNS due to hRSV infection. Moreover, our data indicate that astrocytes can be infected by hRSV suggesting that they could be part of the cellular mechanisms related to CNS inflammation and low hippocampal function. Further, we found an alteration in the permeability to macromolecules and immune cells of the BBB, which is somewhat equivalent to the effect that the West Nile virus produces on the BBB in mice, although hRSV is a much more prevalent pathogen (Roe et al., 2012). Increased BBB permeability to immune cells rises neutrophils, resident macrophages, inflammatory monocytes, B cells, and CD8$^+$ T lymphocytes infiltration into the brains of hRSV-infected mice. As observed in previous studies, inhibition of leukocyte transmigration into the brain by means of CD49d blockade, reduced by 70% viral loads in this tissue (Espinoza et al., 2013). However, the remaining 30% could be due to the virus reaching the brain by alternative routes. Thus, hRSV-infection alters the permeability of the BBB, likely impacting immune cell infiltration into this tissue. Nevertheless, subsequent studies addressing the contribution of the choroid plexus and the immune cells would provide important information for the involvement of nervous-immune interactions during the pathology caused by hRSV (Meeker et al., 2012). Previous studies suggesting possible interactions between the choroid plexus and immune cells (Espinoza et al., 2013) need to be completed by additional research to better understand the contribution to CNS inflammation.

Additionally, increased levels of monocytes infiltrating the CNS have been associated with cognitive impairments and therefore, could be implicated in CNS alterations observed in hRSV-infected mice (Espinoza et al., 2013; Howe et al., 2012). Increased cytokine expression during viral infection can also modulate the normal function of CNS, mainly cognitive processes (Jurgens et al., 2012; Campbell et al., 2010). Here, we found that behavioral alterations caused by hRSV infection lasted up to 60 days p.i., which was manifested by severe digging behavior impairment by the animals and sustained increased expression of IL-4, IL-10, CCL2 and GFAP in the infected animals at this time-point. Our results are in accordance with the observation that the lack of IL-4 increases this type of altered behavior (Moon et al., 2015). While similar findings were described for IL-10 (Mesquita et al., 2008), CCL2 was shown to increase in mice with anxiety-like behavior induced by LPS (Mayerhofer et al., 2017). Together, these results suggest that

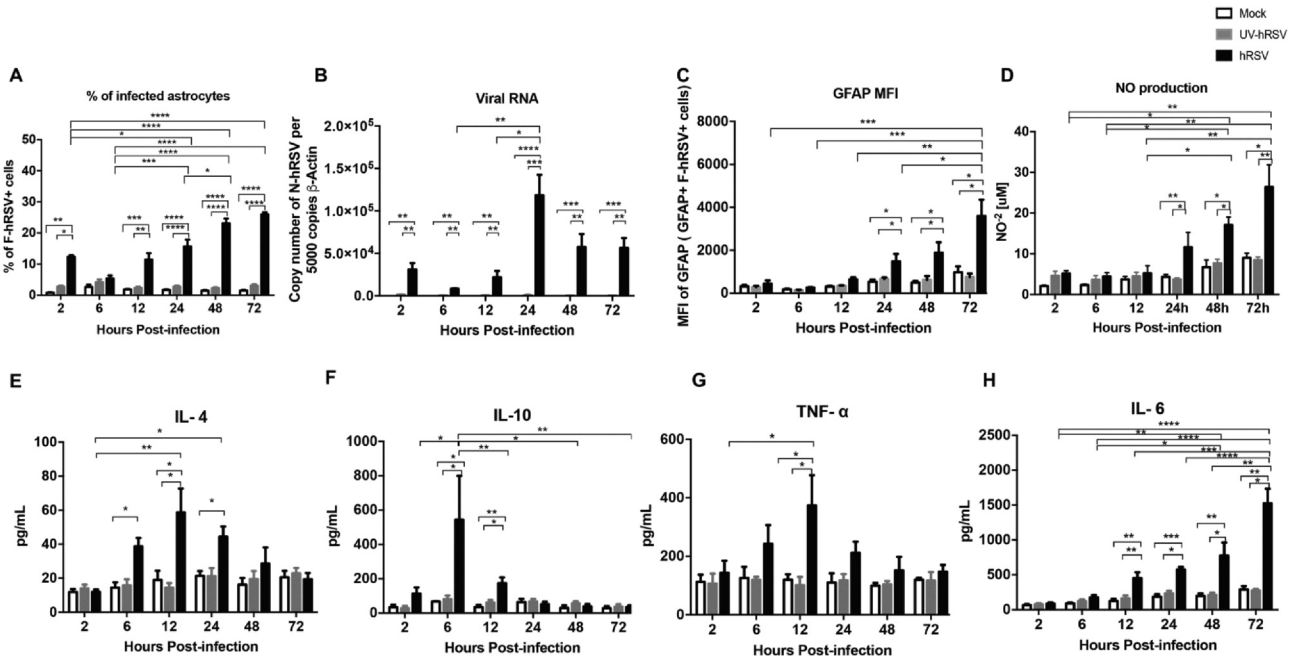

Fig. 8. hRSV infects and activates astrocytes *in vitro*. Primary cultures of mouse astrocytes were infected with hRSV at MOI 5 and cells were analyzed to determine the percentage of F-hRSV$^+$ cells **(a)**, the number of N-hRSV copies analyzed by RT-qPCR **(b),** MFI of GFAP (F-hRSV$^+$ GFAP$^+$) cells **(c)** and the quantification of NO^{-2} in the supernatants of mice astrocytes primary cultures **(d)**. Protein levels of IL-4 **(e)**, IL-10 **(f)**, TNF-α **(g)** and IL-6 **(h)** were evaluated by ELISA. Five independent experiments were performed. Comparisons between groups were performed using a two-way ANOVA test with Bonferronís post-test. **** $P < 0.0001$, *** $P < 0.0005$, ** $P < 0.005$, * $P < 0.05$ indicates that means are significantly different. Bars indicate mean ± SEM.

hRSV infection impairs the normal behavior at extended time-points after infection which is accompanied by an increase of pro-inflammatory cytokines secretion (McAfoose and Baune, 2009; Yirmiya and Goshen, 2011).

Furthermore, studies regarding the effect of influenza (H1N1) infection on spatial learning have shown that despite this virus is not infecting the CNS, peripheral infection induces an increase in mRNA cytokines, such as IL-6, IL-1β and TNF-α, among others (Jurgens et al., 2012). Changes in expression of these cytokines correlated with cognitive impairment observed in the infected mice at day 7 p.i. (Jurgens et al., 2012). Here, we found an increase in the expression of both, IL-6 and TNF-α levels in the brains of hRSV-infected mice, which may have somewhat shared consequences over the CNS. Since hRSV-infection causes an immune response polarized towards a T-helper (Th-) 2 profile, we evaluated IL-4 production and found that the levels of this cytokine were increased during the infection (Fig. 6). These results somewhat suggest that the increase in the expression of these pro-inflammatory cytokines may be due to the activation of microglia and astrocytes, which could be enough to cause a behavioral alteration in mice (Hosseini et al., 2018).

As mentioned above, both CD200 and CX3CL1 are immunomodulatory molecules that are mainly expressed by neurons allowing their interaction with microglia, which express the receptor for these molecules in the resting state (Lyons et al., 2007; Shrivastava et al., 2012; Costello et al., 2011). Also, it is known that CD200-deficient mice display cognitive impairment, suggesting that this molecule plays a significant role in cognition processes (Costello et al., 2011). Similar to what was observed in the brains of influenza-infected mice, we found that CD200 expression was decreased starting day 1p.i. in hRSV-infected mice, while in the study with influenza, this expression was only evaluated on day 7 p.i. (Jurgens et al., 2012). Furthermore, we found a decrease in CX3CL1 mRNA expression in hRSV-infected mice at 3 days p.i. suggesting that the alteration of the normal expression of CD200 and CX3CL1, mainly on day 3p.i., could be due to the activation of microglia with subsequent astrocytes activation and an inflammatory immune response.

Previously, it has been shown that CCL2 attracts inflammatory immune cells to sites of injury, mainly monocytes (Deshmane et al., 2009). In the brain, CCL2 is constitutively expressed by neurons yet, its levels increase in astrocytes and microglia under pathologic conditions (Zhou et al., 2011). In line with the findings of inflammatory monocytes in the brain of hRSV-infected mice, we found that the CCL2 expression was elevated in this tissue. Respiratory virus infection can cause systemic inflammation, as occurs during infection with influenza virus (Jurgens et al., 2012). We evaluated cytokine and chemokine levels in the serum of infected animals. Our findings indicate that the inflammation observed in the brains of hRSV-infected mice is a local effect of hRSV-infection and not due to high levels of systemic cytokines differentiating itself with the influenza virus. Regarding type-I to IFNs expression, we observed a significant decrease in mRNA levels for IFN-α and IFN-β in the brains of hRSV-infected mice, which is consistent with the notion that hRSV can inhibit the production of type-I IFNs to promote viral infection (Spann et al., 2004). These results suggest that the down-regulation of type-I IFNs observed could be due to direct infection of CNS cells by hRSV, which differs from the findings made with influenza. Previously we described that hRSV can be detected in the CNS (Espinoza et al., 2013); yet the cells type targeted by the virus were unknown. Astrocytes are essential players in the cognitive process because the structure of the neuronal synapse depends on the signal pathways mediated by these cells and alterations in astrocytes could eventually contribute to cognitive and behavioral impairments (Volterra and Meldolesi, 2005). In this work, we found that astrocytes which is one of the most abundant cell type in the CNS (Farina et al., 2007; Sofroniew and Vinters, 2010) can be infected by hRSV. These observations have been reported for different viruses, such as the Venezuelan Equine Encephalitis virus (VEE) (Schoneboom et al., 1999), the Sindbis virus (SV) (Brodie et al., 1997), and the Tick-borne Encephalitis virus (TBEV) (Potokar et al., 2014). In virus-infected astrocytes, the production of pro-inflammatory cytokines was induced, as well as the production of NO and GFAP (Brahmachari et al., 2006; Yu et al., 2009). Our results showed co-localization between the F-hRSV protein and GFAP in the cortex, indicating that hRSV can infect

astrocytes *in vivo* (Fig. 7). Such a response is likely to promote inflammation in the CNS and may also cause the activation of microglia. These cells in turn will secrete pro-inflammatory cytokines affecting CNS function (Smith et al., 2012). To definitely determine the cerebral location of immune cells, additional immunohistochemistry and immunofluorescence studies need to be performed. This is an important question to be addressed by future studies, as it goes beyond the scope of this manuscript. Additionally, we found that not only astrocytes colocalized with hRSV antigens (about 5%), but also did 1% of endothelial cells, 1% of microglia cells and 1% of neurons (Fig. 7). Regarding to that, it was previously shown that hRSV can infect 5% of lung neuronal cells and cortical neurons in culture (Li et al., 2006). Moreover, despite the low percentage of hRSV-infected endothelial cells, these infected cells could enhance BBB permeability allowing the transmigration of immune cells into the brain. The infection of microglia also could contribute to the increased amounts of cytokines found in the brains of hRSV-infected mice. The detection of "free" virus probably is associated to the immune cells that infiltrate the CNS of hRSV-infected mice. Nevertheless, additional studies would be needed to better understanding the effects of hRSV-infection on other CNS cell types.

Based on the important role that astrocytes play in several CNS functions, the response of astrocytes to hRSV infection was assayed by astrocyte infection *in vitro* and their responses upon viral challenge. To approach this goal, primary glial cultures were used, which were separated into microglia and astrocytes. Importantly, similar to the observations *in vivo,* we found that astrocyte cultures are permissive to hRSV infection and up-regulate GFAP upon infection. These results are consistent with similar responses seen for astrocyte primary cultures infected with the Junin virus described by others (Pozner, 2008). Additionally, we observed that hRSV-infected astrocytes had a pro-inflammatory profile response characterized by increased production of IL-4, TNF-α and IL-6. These data suggest that hRSV-infection induces murine astrocyte activation and inflammatory responses by secreting pro-inflammatory cytokines, likely involving these cells in neuroinflammation to hRSV infection observed in the animal model. However, our results suggest that hRSV replication may be somewhat impaired in astrocytes as viral RNA was found to decrease over time. Taken together, our work provides new insights onto the effects of hRSV over the CNS and calls for attention to further assess the effects that this virus may have over the brain and its function in humans.

Authors contributions

KB, CR and AK designed the research. KB, JS, CA, AF, JE, MR, and MO performed the experiments; KB and AK wrote the manuscript; JS,CA, MO, AF, MR, EE, PG, and CR reviewed the manuscript and AK reviewed and approved the version to be published. All authors listed have made substantial and intellectual contribution to the work.

Declaration of Competing Interest

The authors declare that they have no known competing financial interests or personal relationships that could have appeared to influence the work reported in this paper.

Acknowledgments

This work was supported by the Millennium Institute on Immunology and Immunotherapy from Chile (P09/016-F for PG, CR and AMK), CONICYT/FONDECYT POSTDOCTORADO No. 3185070 for KB and No. 3190590 for JS. FONDECYT grants number: 1150862, 1190830, 11180739, 1190864 and 1131900.

Appendix A. Supplementary data

Supplementary data to this article can be found online at https://doi.org/10.1016/j.bbi.2020.09.021.

References

Anderson, M.A., Ao, Y., Sofroniew, M.V., 2014. Heterogeneity of reactive astrocytes. Neurosci. Lett. 565, 23–29.
Antonucci, R., Fanos, V., 2005. Acute encephalopathy associated with respiratory syncytial virus infections in childhood. A literature review. Minerva Pediatr. 57, 137–142.
Avital, A., Goshen, I., Kamsler, A., Segal, M., Iverfeldt, K., Richter-Levin, G., Yirmiya, R., 2003. Impaired interleukin-1 signaling is associated with deficits in hippocampal memory processes and neural plasticity. Hippocampus 13 (7), 826–834.
Balschun, D., Wetzel, W., Rey, A., Pitossi, F., Schneider, H., Zuschratter, W., Besedovsky, H.O., 2004. Interleukin-6: a cytokine to forget. FASEB J. 18 (14), 1788–1790.
Bernard-Valnet, R., et al., 2020. Two patients with acute meningoencephalitis concomitant with SARS-CoV-2 infection. Eur. J. Neurol.
Bertollini, C., Ragozzino, D., Gross, C., Limatola, C., Eusebi, F., 2006. Fractalkine/CX3CL1 depresses central synaptic transmission in mouse hippocampal slices. Neuropharmacology 51 (4), 816–821.
Bohmwald, K., et al., 2019. Contribution of Cytokines to Tissue Damage During Human Respiratory Syncytial Virus Infection. Front. Immunol. 10, 452.
Bohmwald, K., Espinoza, J.A., González, P.A., Bueno, S.M., Riedel, C.A., Kalergis, A.M., 2014. Central nervous system alterations caused by infection with the human respiratory syncytial virus: hRSV infection in CNS. Rev. Med. Virol. 24 (6), 407–419.
Bohmwald, K., Galvez, N.M.S., Rios, M., Kalergis, A.M., 2018. Neurologic Alterations Due to Respiratory Virus Infections. Front. Cell. Neurosci. 12, 386.
Brahmachari, S., Fung, Y.K., Pahan, K., 2006. Induction of Glial Fibrillary Acidic Protein Expression in Astrocytes by Nitric Oxide. J. Neurosci. 26, 4930–4939.
Brenner, M., 2014. Role of GFAP in CNS injuries. Neurosci. Lett. 565, 7–13.
Brodie, C., Weizman, N., Katzoff, A., Lustig, S., Kobiler, D., 1997. Astrocyte activation by Sindbis virus: Expression of GFAP, cytokines, and adhesion molecules. Glia 19 (4), 275–285.
Buskila, Y., Farkash, S., Hershfinkel, M., Amitai, Y., 2005. Rapid and reactive nitric oxide production by astrocytes in mouse neocortical slices. Glia 52 (3), 169–176.
Calvo, C., García-García, M.L., Blanco, C., Vázquez, M.C., Frías, M.E., Pérez-Breña, P., Casas, I., 2008. Multiple simultaneous viral infections in infants with acute respiratory tract infections in Spain. J. Clin. Virol. 42 (3), 268–272.
Campbell, I.L., Hofer, M.J., Pagenstecher, A., 2010. Transgenic models for cytokine-induced neurological disease. Biochim. Biophys. Acta (BBA) – Mol. Basis Dis. 1802 (10), 903–917.
Carter, M., Shieh, J., 2015. In: Guide to Research Techniques in Neuroscience (Second Edition). (Academic Press, San Diego, pp. 39–71.
Céspedes, P.F., Rey-Jurado, E., Espinoza, J.A., Rivera, C.A., Canedo-Marroquín, G., Bueno, S.M., Kalergis, A.M., 2017. A single, low dose of a cGMP recombinant BCG vaccine elicits protective T cell immunity against the human respiratory syncytial virus infection and prevents lung pathology in mice. Vaccine 35 (5), 757–766.
Cha, T., Choi, Y.J., Oh, J.-W., Kim, C.-R., Park, D.W., Seol, I.J., Moon, J.-H., 2019. Respiratory syncytial virus-associated seizures in Korean children, 2011–2016. Korean J. Pediatr. 62 (4), 131–137.
Costello, D.A., Lyons, A., Denieffe, S., Browne, T.C., Cox, F.F., Lynch, M.A., 2011. Long Term Potentiation Is Impaired in Membrane Glycoprotein CD200-deficient Mice: A ROLE FOR Toll-LIKE RECEPTOR ACTIVATION. J. Biol. Chem. 286 (40), 34722–34732.
Deacon, R.M.J., 2006. Digging and marble burying in mice: simple methods for in vivo identification of biological impacts. Nat. Protoc. 1 (1), 122–124.
Deacon, R.M.J., Rawlins, J.N.P., 2005. Hippocampal lesions, species-typical behaviours and anxiety in mice. Behav. Brain Res. 156 (2), 241–249.
R. M. J. Deacon. (2009).
Deshmane, S.L., Kremlev, S., Amini, S., Sawaya, B.E., 2009. Monocyte Chemoattractant Protein-1 (MCP-1): An Overview. J. Interferon Cytokine Res. 29 (6), 313–326.
Divarathne, M., Ahamed, R., Noordeen, F., 2019. The Impact of RSV-Associated Respiratory Disease on Children in Asia. J. Pediatr. Infect. Dis. 14 (03), 079–088.
Dong, Y., Benveniste, E.N., 2001. Immune function of astrocytes. Glia 36 (2), 180–190.
Donzis, E.J., Tronson, N.C., 2014. Modulation of learning and memory by cytokines: Signaling mechanisms and long term consequences. Neurobiol. Learn. Mem. 115, 68–77.
Eisenhut, M., 2006. Extrapulmonary manifestations of severe respiratory syncytial virus infection–a systematic review. Crit. Care 10, R107.
Eisenhut, M., 2007. Cerebral involvement in respiratory syncytial virus disease. Brain Dev. 29 (7), 454. https://doi.org/10.1016/j.braindev.2006.11.007.
Eng, L.F., Ghirnikar, R.S., 1994. GFAP and Astrogliosis. Brain Pathol. 4 (3), 229–237.
Espinoza, J.A., Bohmwald, K., Cespedes, P.F., Gomez, R.S., Riquelme, S.A., Cortes, C.M., Valenzuela, J.A., Sandoval, R.A., Pancetti, F.C., Bueno, S.M., Riedel, C.A., Kalergis, A.M., 2013. Impaired learning resulting from Respiratory Syncytial Virus infection. Proc. Natl. Acad. Sci. 110 (22), 9112–9117.
Farina, C., Aloisi, F., Meinl, E., 2007. Astrocytes are active players in cerebral innate immunity. Trends Immunol. 28 (3), 138–145.
Flores, B., von Bernhardi, R., 2012. Transforming growth factor beta1 modulates amyloid beta-induced glial activation through the Smad3-dependent induction of MAPK phosphatase-1. J. Alzheimers Dis. 32, 417–429.
Gomez, R.S., et al., 2016. Contribution of Fcgamma receptors to human respiratory syncytial virus pathogenesis and the impairment of T-cell activation by dendritic cells. Immunology 147, 55–72.
Greter, M., Lelios, I., Croxford, A.L., 2015. Microglia Versus Myeloid Cell Nomenclature during Brain Inflammation. Front. Immunol. 6 (249).

Griffith, J.W., Sokol, C.L., Luster, A.D., 2014. Chemokines and Chemokine Receptors: Positioning Cells for Host Defense and Immunity. Annu. Rev. Immunol. 32 (1), 659–702.
Hansen, R., et al., 2001. Activation of microglia cells is dispensable for the induction of rat retroviral spongiform encephalopathy. J. Neurovirol. 7 (6), 501–510.
Hornuss, D., et al., 2020. Anosmia in COVID-19 patients. Clin. Microbiol. Infect.
Hosseini, S., Wilk, E., Michaelsen-Preusse, K., Gerhauser, I., Baumgärtner, W., Geffers, R., Schughart, K., Korte, M., 2018. Long-Term Neuroinflammation Induced by Influenza A Virus Infection and the Impact on Hippocampal Neuron Morphology and Function. J. Neurosci. 38 (12), 3060–3080.
Howe, C.L., LaFrance-Corey, R.G., Sundsbak, R.S., LaFrance, S.J., 2012. Inflammatory monocytes damage the hippocampus during acute picornavirus infection of the brain. J. Neuroinflammation 9 (1). https://doi.org/10.1186/1742-2094-9-50.
Jang, H., Boltz, D., Sturm-Ramirez, K., Shepherd, K.R., Jiao, Y., Webster, R., Smeyne, R.J., 2009. Highly pathogenic H5N1 influenza virus can enter the central nervous system and induce neuroinflammation and neurodegeneration. Proc. Natl. Acad. Sci. 106 (33), 14063–14068.
Jones, B.A., Beamer, M., Ahmed, S., 2010. Fractalkine/CX3CL1: A Potential New Target for Inflammatory Diseases. Mol. Interventions 10 (5), 263–270.
Jurgens, H.A., Amancherla, K., Johnson, R.W., 2012. Influenza Infection Induces Neuroinflammation, Alters Hippocampal Neuron Morphology, and Impairs Cognition in Adult Mice. J. Neurosci. 32 (12), 3958–3968.
Kawashima, H., Ioi, H., Ushio, M., Yamanaka, G., Matsumoto, S., Nakayama, T., 2009. Cerebrospinal fluid analysis in children with seizures from respiratory syncytial virus infection. Scand. J. Infect. Dis. 41 (3), 228–231.
Kawashima, H., Kashiwagi, Y., Ioi, H., Morichi, S., Oana, S., Yamanaka, G., Takekuma, K., Hoshika, A., Sawai, J., Kato, Y., 2012. Production of chemokines in respiratory syncytial virus infection with central nervous system manifestations. J. Infect. Chemother. 18 (6), 827–831.
Kho, N., Kerrigan, J.F., Tong, T., Browne, R., Knilans, J., 2004. Respiratory Syncytial Virus Infection and Neurologic Abnormalities: Retrospective Cohort Study. J. Child Neurol. 19 (11), 859–864.
Lange, S.C., Bak, L.K., Waagepetersen, H.S., Schousboe, A., Norenberg, M.D., 2012. Primary Cultures of Astrocytes: Their Value in Understanding Astrocytes in Health and Disease. Neurochem. Res. 37 (11), 2569–2588.
Lauro, C., Catalano, M., Trettel, F., Limatola, C., 2015. Fractalkine in the nervous system: neuroprotective or neurotoxic molecule? Ann. N. Y. Acad. Sci. 1351, 141–148.
Li, X.-Q., Fu, Z.F., Alvarez, R., Henderson, C., Tripp, R.A., 2006. Respiratory Syncytial Virus (RSV) Infects Neuronal Cells and Processes That Innervate the Lung by a Process Involving RSV G Protein. JVI 80 (1), 537–540.
Lyons, A., Downer, E.J., Crotty, S., Nolan, Y.M., Mills, K.H.G., Lynch, M.A., 2007. CD200 Ligand Receptor Interaction Modulates Microglial Activation In Vivo and In Vitro: A Role for IL-4. J. Neurosci. 27 (31), 8309–8313.
Mao, L., Jin, H., Wang, M., Hu, Y.u., Chen, S., He, Q., Chang, J., Hong, C., Zhou, Y., Wang, D., Miao, X., Li, Y., Hu, B.o., 2020. Neurologic Manifestations of Hospitalized Patients With Coronavirus Disease 2019 in Wuhan, China. JAMA Neurol 77 (6), 683.
Mayerhofer, R., Fröhlich, E.E., Reichmann, F., Farzi, A., Kogelnik, N., Fröhlich, E., Sattler, W., Holzer, P., 2017. Diverse action of lipoteichoic acid and lipopolysaccharide on neuroinflammation, blood-brain barrier disruption, and anxiety in mice. Brain Behav. Immun. 60, 174–187.
McAfoose, J., Baune, B.T., 2009. Evidence for a cytokine model of cognitive function. Neurosci. Biobehav. Rev. 33 (3), 355–366.
Meeker, R.B., Williams, K., Killebrew, D.A., Hudson, L.C., 2012. Cell trafficking through the choroid plexus. Cell Adh. Migr. 6 (5), 390–396.
Meinhardt, J., et al., 2020. Olfactory transmucosal SARS-CoV-2 invasion as port of Central Nervous System entry in COVID-19 patients. bioRxiv 2020.2006.2004.135012.
Mesquita, A.R., Correia-Neves, M., Roque, S., Castro, A.G., Vieira, P., Pedrosa, J., Palha, J.A., Sousa, N., 2008. IL-10 modulates depressive-like behavior. J. Psychiatr. Res. 43 (2), 89–97.
Middeldorp, J., Hol, E.M., 2011. GFAP in health and disease. Prog. Neurobiol. 93 (3), 421–443.
Millichap, J.J., Wainwright, M.S., 2009. Neurological Complications of Respiratory Syncytial Virus Infection: Case Series and Review of Literature. J. Child Neurol. 24 (12), 1499–1503.
Miner, J.J., Diamond, M.S., 2016. Mechanisms of restriction of viral neuroinvasion at the blood–brain barrier. Curr. Opin. Immunol. 38, 18–23.
Moon, M.L., Joesting, J.J., Blevins, N.A., Lawson, M.A., Gainey, S.J., Towers, A.E., McNeil, L.K., Freund, G.G., 2015. IL-4 Knock Out Mice Display Anxiety-Like Behavior. Behav. Genet. 45 (4), 451–460.
Morichi, S., Kawashima, H., Ioi, H., Yamanaka, G., Kashiwagi, Y., Hoshika, A., Nakayama, T., Watanabe, Y., 2011. Classification of acute encephalopathy in respiratory syncytial virus infection. J. Infect. Chemother. 17 (6), 776–781.
Morichi, S., Morishita, N., Ishida, Y.u., Oana, S., Yamanaka, G., Kashiwagi, Y., Kawashima, H., 2017. Examination of neurological prognostic markers in patients with respiratory syncytial virus-associated encephalopathy. Int. J. Neurosci. 127 (1), 44–50.
Moriguchi, T., Harii, N., Goto, J., Harada, D., Sugawara, H., Takamino, J., Ueno, M., Sakata, H., Kondo, K., Myose, N., Nakao, A., Takeda, M., Haro, H., Inoue, O., Suzuki-Inoue, K., Kubokawa, K., Ogihara, S., Sasaki, T., Kinouchi, H., Kojin, H., Ito, M., Onishi, H., Shimizu, T., Sasaki, Y.u., Enomoto, N., Ishihara, H., Furuya, S., Yamamoto, T., Shimada, S., 2020. A first case of meningitis/encephalitis associated with SARS-Coronavirus-2. Int. J. Infect. Dis. 94, 55–58.
Ng, Y.-T., Cox, C., Atkins, J., Butler, I.J., 2001. Encephalopathy Associated With Respiratory Syncytial Virus Bronchiolitis. J. Child Neurol. 16 (2), 105–108.
Obodai, E., et al., 2018. The significance of human respiratory syncytial virus (HRSV) in children from Ghana with acute lower respiratory tract infection: A molecular epidemiological analysis, 2006 and 2013–2014. PLoS ONE 13, e0203788.
Otake, Y., Yamagata, T., Morimoto, Y., Imi, M., Mori, M., Aihara, T., Ichiyama, T., Momoi, M.Y., 2007. Elevated CSF IL-6 in a patient with respiratory syncytial virus encephalopathy. Brain Dev. 29 (2), 117–120.
Pfaffl, M.W., 2001. A new mathematical model for relative quantification in real-time RT-PCR. *Nucleic Acids Res* 29, e45.
Picone, S., Mondì, V., Di Palma, F., Martini, L., Paolillo, P., 2019. Neonatal Encephalopathy and SIADH during RSV Infection. Am. J. Perinatol. 36 (S 02), S106–S109.
Potokar, M., Korva, M., Jorgacevski, J., Avsic-Zupanc, T., Zorec, R., 2014. Tick-borne encephalitis virus infects rat astrocytes but does not affect their viability. PLoS One 9, e86219.
Pozner, R.G., et al., 2008. Astrocyte response to Junin virus infection. Neurosci. Lett. 445, 31–35.
Puntambekar, S.S., Davis, D.S., Hawel III, L., Crane, J., Byus, C.V., Carson, M.J., 2011. LPS-induced CCL2 expression and macrophage influx into the murine central nervous system is polyamine-dependent. Brain Behav. Immun. 25 (4), 629–639.
Ransohoff, R.M., Cardona, A.E., 2010. The myeloid cells of the central nervous system parenchyma. Nature 468 (7321), 253–262.
Roe, K., et al., 2012. West Nile virus-induced disruption of the blood-brain barrier in mice is characterized by the degradation of the junctional complex proteins and increase in multiple matrix metalloproteinases. J. Gener. Virol. 93, 1193–1203.
Rogers, J.P., Chesney, E., Oliver, D., Pollak, T.A., McGuire, P., Fusar-Poli, P., Zandi, M.S., Lewis, G., David, A.S., 2020. Psychiatric and neuropsychiatric presentations associated with severe coronavirus infections: a systematic review and meta-analysis with comparison to the COVID-19 pandemic. Lancet Psych. 7 (7), 611–627.
Santello, M., Volterra, A., 2012. TNFalpha in synaptic function: switching gears. Trends Neurosci. 35, 638–647.
Schildge, S., Bohrer, C., Beck, K., Schachtrup, C., 2013. Isolation and culture of mouse cortical astrocytes. J. Vis. Exp.
Schneider, C.A., Rasband, W.S., Eliceiri, K.W., 2012. NIH Image to ImageJ: 25 years of image analysis. Nat Methods 9, 671–675.
Schoneboom, B.A., Fultz, M.J., Miller, T.H., McKinney, L.C., Grieder, F.B., 1999. Astrocytes as targets for Venezuelan equine encephalitis virus infection. J. Neurovirol. 5 (4), 342–354.
Seibenhener, M.L., Wooten, M.C., 2015. Use of the Open Field Maze to measure locomotor and anxiety-like behavior in mice. J. Vis. Exp. e52434.
Shrivastava, K., Gonzalez, P., Acarin, L., 2012. The immune inhibitory complex CD200/CD200R is developmentally regulated in the mouse brain. J. Comp. Neurol. 520 (12), 2657–2675.
Smith, J.A., Das, A., Ray, S.K., Banik, N.L., 2012. Role of pro-inflammatory cytokines released from microglia in neurodegenerative diseases. Brain Res. Bull. 87 (1), 10–20.
Sofroniew, M.V., Vinters, H.V., 2010. Astrocytes: biology and pathology. Acta Neuropathol. 119 (1), 7–35.
Spann, K.M., Tran, K.C., Chi, B., Rabin, R.L., Collins, P.L., 2004. Suppression of the induction of alpha, beta, and lambda interferons by the NS1 and NS2 proteins of human respiratory syncytial virus in human epithelial cells and macrophages [corrected]. J. Virol. 78, 4363–4369.
Sweetman, L.L., Ng, Y.-T., Butler, I.J., Bodensteiner, J.B., 2005. Neurologic Complications Associated With Respiratory Syncytial Virus. Pediatr. Neurol. 32 (5), 307–310.
Takeuchi, R., Tsutsumi, H., Osaki, M., Sone, S., Imai, S., Chiba, S., 1998. Respiratory Syncytial Virus Infection of Neonatal Monocytes Stimulates Synthesis of Interferon Regulatory Factor 1 and Interleukin-1β (IL-1β)-Converting Enzyme and Secretion of IL-1β. J. Virol. 72 (1), 837–840.
T. Tanaka M. Narazaki T. Kishimoto IL-6 in Inflammation, Immunity, and Disease Cold Spring Harbor Perspect. Biol. 6 a016295 2014.
Thomas, A., Burant, A., Bui, N., Graham, D., Yuva-Paylor, L.A., Paylor, R., 2009. Marble burying reflects a repetitive and perseverative behavior more than novelty-induced anxiety. Psychopharmacology 204 (2), 361–373.
Torres, J.P., Gomez, A.M., Khokhar, S., Bhoj, V.G., Tagliabue, C., Chang, M.L., Kiener, P.A., Revell, P.A., Ramilo, O., Mejias, A., 2010. Respiratory Syncytial Virus (RSV) RNA loads in peripheral blood correlates with disease severity in mice. Respir. Res. 11 (1).
Varatharaj, A., Galea, I., 2017. The blood-brain barrier in systemic inflammation. Brain Behav. Immun. 60, 1–12.
Volterra, A., Meldolesi, J., 2005. Astrocytes, from brain glue to communication elements: the revolution continues. Nat. Rev. Neurosci. 6 (626).
Wang, C., et al., 2019. Ventral Hippocampus Modulates Anxiety-Like Behavior in Male But Not Female C57BL/6J Mice. Neuroscience 418, 50–58.
Yirmiya, R., Goshen, I., 2011. Immune modulation of learning, memory, neural plasticity and neurogenesis. Brain Behav. Immun. 25 (2), 181–213.
Yu, D., Zhu, H., Liu, Y., Cao, J., Zhang, X., 2009. Regulation of proinflammatory cytokine expression in primary mouse astrocytes by coronavirus infection. J. Virol. 83, 12204–12214.
Zhivaki, D., Lemoine, S., Lim, A., Morva, A., Vidalain, P.-O., Schandene, L., Casartelli, N., Rameix-Welti, M.-A., Hervé, P.-L., Dériaud, E., Beitz, B., Ripaux-Lefevre, M., Miatello, J., Lemercier, B., Lorin, V., Descamps, D., Fix, J., Eléouët, J.-F., Riffault, S., Schwartz, O., Porcheray, F., Mascart, F., Mouquet, H., Zhang, X., Tissières, P., Lo-Man, R., 2017. Respiratory Syncytial Virus Infects Regulatory B Cells in Human Neonates via Chemokine Receptor CX3CR1 and Promotes Lung Disease Severity. Immunity 46 (2), 301–314.
Zhou, Y., Tang, H., Liu, J., Dong, J., Xiong, H., 2011. Chemokine CCL2 modulation of neuronal excitability and synaptic transmission in rat hippocampal slices. J. Neurochem. 116, 406–414.
Zlateva, K.T., Van Ranst, M., 2004. Detection of subgroup B respiratory syncytial virus in the cerebrospinal fluid of a patient with respiratory syncytial virus pneumonia. Pediatr. Infect. Dis. J. 23 (11), 1065–1066.